

***Optimizing The Detection Of Neutrons From Small-Quantity  
Weapons-Grade Nuclear Materials***

A paper presented

by

***Craig-Alan C. Bias, Major, USAF, BSC***

to

*The Department of Radiological Health Sciences*

in partial fulfillment of the requirements

for the degree of

***Master of Science***

in the subject of

***Health Physics***

Colorado State University

Fort Collins, Colorado

**May 2002**

## TABLE OF CONTENTS

INTRODUCTION	1
BACKGROUND	3
Neutron Classification and Sources	3
Neutron Detection	5
Neutron Transport Modeling	8
Weapons-Grade Nuclear Materials	9
MATERIALS AND METHODS	11
Neutron Yields and Energy Distributions of Weapons-Grade Nuclear Materials	11
Laboratory Neutron Source	14
Cylindrical BF <sub>3</sub> Detectors	15
Evaluation of MCNP Functions Using Spherical BF <sub>3</sub>	16
Evaluation of Modeling Accuracy Using LND 201 BF <sub>3</sub>	17
Use of MCNP to Model Detection of Weapons-Grade Nuclear Material in Checked Baggage	18
RESULTS AND DISCUSSION	21
Watts Thermal Neutron-Induced Fission Spectrum of Pu-239	21
Evaluation of MCNP Functions Using Spherical BF <sub>3</sub>	22
Pencil Beam Neutron Source	22
Plane Parallel Beam Neutron Source	29
Isotropic Point Neutron Source	35
Validation of MCNP Accuracy Using LND 201 BF <sub>3</sub>	41
Lucite Moderator	41
Lucite and Lead or Carbon Moderator	49
Use of MCNP to Model Detection of Weapons-Grade Nuclear Material in Checked Baggage	52
CONCLUSION	58
Summary of Data	58
Considerations for Future Efforts	60
BIBLIOGRAPHY	62

## INTRODUCTION

The threat of nuclear materials being used to inflict physical and/or psychological effects on the populace drives the United States policy of non-proliferation enforcement. Non-proliferation strives to hinder such incidents by ensuring storage and disposition methods prevent unauthorized parties from obtaining weapons-usable nuclear materials. Since non-proliferation is a policy of prevention, it must rely on the detection of such nuclear materials, often in small quantities, before they have been used in constructing a weapon. Generally, one can detect either the gamma radiation or the neutrons resulting from the nuclear material as it decays and/or interacts with its environment. Weapons-usable nuclear materials mostly emit infrequent, low-energy gamma radiation that is difficult to detect reliably amidst frequent and highly variable background levels of gamma radiation. In contrast, they can also be prolific sources of neutrons that can reliably be detected amidst very low background levels of neutrons.

Non-proliferation efforts focus on a class of nuclear material called “fissile material” or specifically any material fissionable by thermal neutrons (Shleien 1998). While all fissile materials are weapons-useable, plutonium-239 and uranium-235 are the most desired weapons-usable fissile materials due to their low rates of spontaneous fission (DOE 1997). In 1997, the United States alone declared 250 tons of weapons-usable fissile materials as excess, including 58 tons of plutonium and 192 tons of highly enriched uranium (HEU) (Albright 1999). The Department of Energy classifies the threats to these fissile materials as either “host state diversion or recovery” or as “theft by unauthorized parties” (DOE 1997). Theft of weapons-usable fissile materials from research facilities, nuclear facilities or past military disposal sites poses a continued and

realistic threat worldwide. Therefore, non-proliferation must include theft prevention and the subsequent detection of these material should they be stolen.

The purpose of this project was to examine the feasibility of reliably detecting neutrons produced by small quantities of weapons-grade nuclear materials should they be transported in baggage that would be screened at airports within the United States. Plutonium-239, weapons-grade plutonium (WGP), uranium-235, and weapons-grade uranium (WGU) were modeled. Calculations were made of the neutron detection rates above expected neutron background rates through laboratory measurements using a boron trifluoride ( $\text{BF}_3$ ) proportional counter and through modeling using Monte Carlo methods.

## BACKGROUND

### Neutron Classification and Sources

Neutrons are generally classified by their energies. At very low energies, a neutron can reach an energy state where the neutron is in thermal equilibrium with its surroundings and hence classified a “thermal neutron” (Shleien 1998) with a most probable energy of 0.0025 eV at room temperature (20°C). These thermal neutrons gain and lose little energy through interactions with matter and diffuse about randomly until captured, or absorbed, by a nucleus. Once capture occurs, the nucleus becomes unstable, leading to competing stabilizing reactions such as (n,p), (n,2n), (n, $\alpha$ ), or (n, $\gamma$ ).

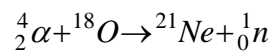
There are several methods by which neutrons may be produced: spontaneous fission, induced fission, or  $\alpha$ -particle induced reactions. Very heavy radioactive isotopes, whose atomic number (Z) and atomic mass number (A) are such that  $Z^2/A \geq 49$ , may undergo spontaneous fission (SF). That is, under certain conditions, the nucleus may become highly deformed and split into two smaller nuclei, called fission fragments, and several neutrons (Cember 1996). In these heavy nuclei, spontaneous fission competes with radioactive decay as a stabilizing process. Neutrons from spontaneous fission are emitted with a Maxwellian energy distribution given by the equation:

$$N(E)dE = \sqrt{E} \exp(-E/0.143) dE$$

where  $N(E)dE$  is the number of neutrons emitted with energy E, in energy interval dE, in units of MeV (DOE 2000).

In contrast to these spontaneous processes, some materials can be made to fission when exposed to neutrons. “Fissile” materials, such as U-235 and Pu-239, may fission upon capturing a thermal neutron and this process is thereby referred to as “induced fission.” Neutrons from induced fission are also emitted with a Maxwellian energy distribution (Canberra 2002). Of the fissile materials, uranium-233, uranium-235 and plutonium-239 are the only isotopes considered practical for use as fission explosives. Uranium-233 however has very high rates of gamma and neutron emissions that make its handling and use difficult, leaving U-235 and Pu-239 as the primary isotopes of interest (Sublette 1999).

All radioactive isotopes undergo radioactive decay, or spontaneous nuclear transformations, to become more stable elements. Plutonium and uranium isotopes decay by  $\alpha$ -emission. The  $\alpha$ -particle may be subsequently absorbed by the nuclei of low atomic number elements, such as oxygen, and a neutron produced by the following ( $\alpha$ , n) reaction:



Unlike spontaneous fission and induced fission, neutrons from ( $\alpha$ , n) reactions are not emitted with a Maxwellian energy distribution. Their energy distribution varies according to the geometries involved as the  $\alpha$ -particle and target nucleus (oxygen in the above reaction) interact in those geometries.

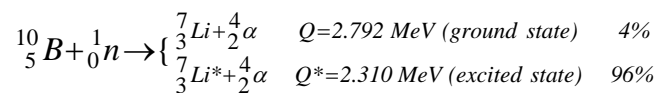
## Neutron Detection

Neutrons are not directly ionizing and therefore cannot be detected directly. They must react with another medium to produce an ionizing particle that can be detected (Tsoulfanidis 1995). Neutrons originating from spontaneous fission or ( $\alpha$ , n) reactions in fissile materials are classified as fast neutrons with energies from about 0.1 MeV to 10 or 20 MeV. A neutron total cross-section is a target nuclei specific area, measured in barns (1 barn =  $10^{-24}$  cm<sup>2</sup>), in which the incident neutrons are most likely to undergo an interaction (Hartcourt 2002). The total cross-section is the sum of the individual cross-sections for scattering (elastic and inelastic), capture, and induced fission. Because the cross section for neutron interactions in most materials is a function of neutron energy, different detection techniques have been developed for different neutron energy regions (Knoll 2000). The most important process for fast neutron detection is elastic neutron scattering. In this interaction an incident neutron transfers some of its kinetic energy to the target nucleus, resulting in a recoil nucleus. If the target nucleus is hydrogen, a recoil proton results and fast neutrons can be preferentially detected due to the large kinetic energy of the recoil proton. However, the cross-section for elastic scatter is small (20.5 barns) and many of the recoil protons have energies that are too low to be detected. Thus, the sensitive volume of the detector must be large in order to assure that a sufficient signal can be obtained.

Thermal neutron detectors rely on neutron capture cross-sections that release a large amount of energy. The principle behind these detectors is based on slowing down incident fast neutrons in a moderator and then detecting the resulting thermal neutrons with a high cross-section capture reaction. Common detectors based on such reactions

include the boron trifluoride (BF<sub>3</sub>) detector, <sup>6</sup>Li detector, and the <sup>3</sup>He detector. The cross-sections for a (n, charged particle) capture reaction are  $\sigma_c = 3837$  barns for BF<sub>3</sub>,  $\sigma_c = 945$  barns for <sup>6</sup>Li, and  $\sigma_c = 5327$  barns for <sup>3</sup>He (Shleien 1998). Li-based detectors are often based on scintillation techniques (i.e. LiI) that are expensive and require photomultipliers that are often also sensitive to photons. The <sup>3</sup>He cross-section is the highest and since <sup>3</sup>He detectors can be operated at higher gas pressures, they theoretically offer higher detection efficiency than BF<sub>3</sub>. However, <sup>3</sup>He detectors are more sensitive to gamma radiation and result in poor discrimination between thermal neutron pulses and gamma radiation pulses (Knoll 2000).

The BF<sub>3</sub> detector is most practical in this project since the capture cross-section for <sup>10</sup>B is 3837 barns and over 2 MeV of energy is released in the kinetic energy of charged particles that are fairly easy to detect. Additional advantages include the 1/v energy dependence of the cross-section and the dual use of the BF<sub>3</sub> gas as a proportional gas in the counter and as the target atom for the incident neutrons (Tsoulfanidis 1995). An incident thermal neutron interacts with the target boron atom in the BF<sub>3</sub> gas and undergoes the following (n,  $\alpha$ ) reaction:



The <sup>7</sup>Li recoil nucleus and the  $\alpha$ -particle are emitted in opposite directions, with combined energies of either 2.3 MeV or 2.792 MeV, where 96% of the time the lithium nucleus is in an excited state. The energy of the lithium and/or the  $\alpha$ -particle can then be deposited in the BF<sub>3</sub> gas whereby a corresponding pulse height (using a multi-channel analyzer) or pulse (using a single-channel analyzer) is registered (Knoll 2000).

By enriching the  $\text{BF}_3$  gas such that 96% of the boron atoms are  $^{10}\text{B}$  rather than  $^{11}\text{B}$ , the detector efficiency is enhanced about five-fold. This is because the thermal neutron capture cross-section, or probability of capture, for  $^{10}\text{B}$  ( $\sigma_c = 3837$  barns) is  $7.7 \times 10^5$  times higher than for the naturally abundant  $^{11}\text{B}$  ( $\sigma_c = 0.005$  barns). Most gamma radiation interactions result in low-amplitude pulses that lie in the tail smaller than the properly set discriminator. This serves to eliminate gamma radiation without sacrificing neutron detection efficiency (Knoll 2000).

The efficiency for this type of neutron capture detector system can be improved by surrounding the detector with hydrogenous material. The incident fast neutrons can then lose a portion of their kinetic energy through elastic scattering with hydrogen atoms and eventually reach the detector with thermal kinetic energy for which the neutron capture cross section is high. Most importantly, since an incident neutron can transfer up to its entire kinetic energy in a single collision with a hydrogen atom, fast neutrons can be efficiently slowed or “moderated” with hydrogenous materials. As the thickness of this moderator around the detector increases, the number of hydrogen atoms increases as does the number of elastic scattering events. Theoretically, detection efficiency should then increase with increasing moderator thickness. However, the efficiency of a moderated slow neutron detector, when used with a monoenergetic fast neutron source, shows a maximum at a specific moderator thickness. For a common moderator such as polyethylene, this optimum thickness ranges from a few centimeters for keV neutrons up to several tens of centimeters for MeV neutrons (Knoll 2000). Moderators larger than this optimum tend to decrease the detection efficiency because the moderated neutrons have a higher probability of being captured in the moderator rather than in the detector.

In addition, as the detector volume becomes a smaller fraction of the total system volume, there will be a lower probability of a given neutron's path intersecting the detector volume before escaping the system.

### **Neutron Transport Modeling**

The Monte Carlo technique of numerical analysis uses random sampling to construct a solution of mathematical or physical problems. Monte Carlo techniques are commonly used to obtain detailed computer simulations of how neutrons are transported through matter and interact with it. The Monte Carlo n-Particle Transport code (MCNP) developed by Los Alamos National Laboratory is a well-tested code used to model neutron transport. The user specifies the physical and, if applicable, the radiation characteristics of the neutron source, the detectors, the moderators and their environment.

Accurate modeling is essential but not sufficient. The user must specify what information MCNP should produce as a scored result called a "tally." Each particle generated by the source, or by subsequent interaction with matter defined in the problem, is tracked until its history is terminated. Particle histories are typically terminated because the particle escaped the defined boundaries of the problem, was below a specified energy cutoff, was below a specified importance, passed multiple times through a region defined with low importance, or reacted by capture, neutron multiplication, or fission. Variance reduction is important to produce reliable tallies. Many methods are available and the standard techniques prescribed in the MCNP documentation were utilized in this project.

## **Weapons-Grade Nuclear Materials**

Weapons-grade nuclear materials (WGNM) are required for construction of nuclear weapon components and are potential radioactive sources in radiological dispersal devices (RDD). For the purposes of this project, WGNM are defined as those fissile materials that contain at least 93% Pu-239 or 94% U-235 by mass and include 100% Pu-239, weapons-grade plutonium (WGP), 100% U-235, and weapons-grade uranium (WGU). In the United States, WGP is defined as being composed of >93% Pu-239 and the remainder is assumed to be mainly Pu-238 and Pu-240. WGU is defined as being composed of >94% U-235 and the remainder is assumed to be U-234 and U-238 (DOE, 1997).

Pu-239 and U-235 are considered the most useful weapon components due to their very low rates of spontaneous fission. Radioactive materials that may be more useful in RDDs have high spontaneous fission rates, are thereby more easily detected, and are not considered in this project. Highly enriched uranium (HEU) consists of 20-90% U-235 by mass and could also be used as a nuclear device component, although larger quantities would be required than if WGU were used. It is estimated that anyone with sufficient expertise and 15 kg of HEU or 5 kg of WGP could build a primitive nuclear weapon in a few days or weeks. According to a 1995 Natural Resources Defense Council report, nuclear weapons with a destructive power of 1 kton could be built using modern technology with as little as 2.5 kg of HEU or 1 kg of WGP (Chow 1993). As a reference, the Fat Man bomb detonated over Nagasaki was an implosion-type weapon containing 6.1 kg WGP and had a yield of 21 kton. The Little Boy bomb detonated over Hiroshima was a gun-type weapon containing 61.4 kg of HEU (80% U-235) and had an

approximate yield of 15 kton (Sublette 1997). The smallest theoretical critical mass (mass required to sustain a chain reaction) of Pu-239 is only a few hundred grams (Allison 1996). Based on a density of  $19.8 \text{ g/cm}^3$ , 100-g of Pu-239 only occupies the space of a 1.5-cm sided cube...similar to the size of a six-sided playing die.

Plutonium oxidizes slowly in dry air but oxidizes rapidly as the temperature and/or relative humidity increases (DOE 2001). For a relative humidity increase from 0% to 50%, the oxidation rate will increase by several orders of magnitude (EPA 1990). In contrast, uranium oxidizes rapidly in air, typically within hours, to a hard, black surface (DOE 1998). The metal oxides are very stable and as they are formed on the metal surface, they become increasingly prolific sources of fast neutrons due to the ( $\alpha$ , n) reactions.

## MATERIALS AND METHODS

### Neutron Yields and Energy Distributions of Weapons-Grade Nuclear Materials

Specific Yield is defined as the number of neutrons produced per second per gram of nuclear material. While many neutron-producing interactions can occur, those of interest for this project are spontaneous fission (SF), induced fission (n, 2n), and radioactive decay reactions in oxides ( $\alpha$ , n). While the yields for induced fission cannot be predicted without further knowledge of the environments and geometries, the specific yields for (SF) and ( $\alpha$ , n) for selected weapons-grade nuclear materials (WGNM) are presented in Table 1.

**Table 1. Specific Neutron Yields of Select WGNM (DOE 2000)**

WGNM	(SF) Specific Yield (n/sec-g)	( $\alpha$ , n) Specific Yield in Oxides (n/sec-g)	Total Neutron Specific Yield (n/sec-g)
U-235	$2.99 \times 10^{-4}$	$7.1 \times 10^{-4}$	$1.0 \times 10^{-3}$
WGU <sup>1</sup>	$5.11 \times 10^{-4}$	$3.07 \times 10^{-2}$	$3.1 \times 10^{-2}$
Pu-239	$2.18 \times 10^{-2}$	$3.81 \times 10^1$	$3.8 \times 10^1$
WGP <sup>2</sup>	66.4	128	194

<sup>1</sup>Yields based on composition of U-235 (94%), U-234 (1%) and U-238 (5%)

<sup>2</sup>Yields based on composition of Pu-239 (93%), Pu-238 (0.05%), Pu-240 (6.1%), Pu-241 (0.8%) and Pu-242 (0.05%)

Table 1 illustrates that impurities (isotopes other than Pu-239 or U-235) substantially increase the specific neutron yield of the WGNM. If the reciprocal of the specific yield is taken, one obtains the theoretical mass required to produce one neutron per second for that specific yield.

Table 2 reinforces the importance of the ( $\alpha$ , n) reactions in oxides to the total specific yields of plutonium and of uranium. Table 2 also highlights the minute mass of plutonium that may be detected at a given rate when compared to that of uranium.

**Table 2. Calculated Mass Required to Produce One Neutron Per Second in Select WGNM**

WGNM	Calculated Mass (g) Based On (SF) Specific Yield	Calculated Mass (g) Based On ( $\alpha$ , n) Specific Yield	Calculated Mass (g) Based On Total Specific Yield
U-235	3300	1400	1000
WGU	2000	33	32
Pu-239	46	0.026	0.026
WGP	0.015	0.008	0.005

As stated earlier, neutrons resulting from both spontaneous fission and induced fission reactions are characterized by a Maxwell energy distribution. In the use of MCNP, the Watts fission spectrum is used as an alternative to the Maxwell fission spectrum for induced fission of both Pu-239 and U-235. The Watts fission spectrum is modeled by the following equation:

$$N(E)dE = \exp(-E/a) \sinh(\sqrt{b * E}) dE$$

where  $N(E)dE$  is the number of neutrons emitted with energy  $E$  in the energy interval  $dE$  in units of MeV. The coefficients  $a$  and  $b$  for induced fission of U-235 by thermal neutrons are  $a = 0.988$  MeV and  $b = 2.249$  MeV<sup>-1</sup>. The coefficients  $a$  and  $b$  for induced fission of Pu-239 by thermal neutrons are  $a = 0.966$  MeV and  $b = 2.842$  MeV<sup>-1</sup> (Briesmeister 2000, App. H).

Literature commonly references the use of Maxwell distributions to represent neutron spectra. In the use of MCNP, a Watts distribution is used as an alternative representation of the neutron spectra. Figure 1 compares a Maxwell neutron spectrum to Watts neutron spectra for U-235 and for Pu-239. The area under each curve was normalized to unity. Since there is excellent agreement between the Maxwell and Watts spectrum for these fissile materials, the Watts distribution was used in the remainder of this project.

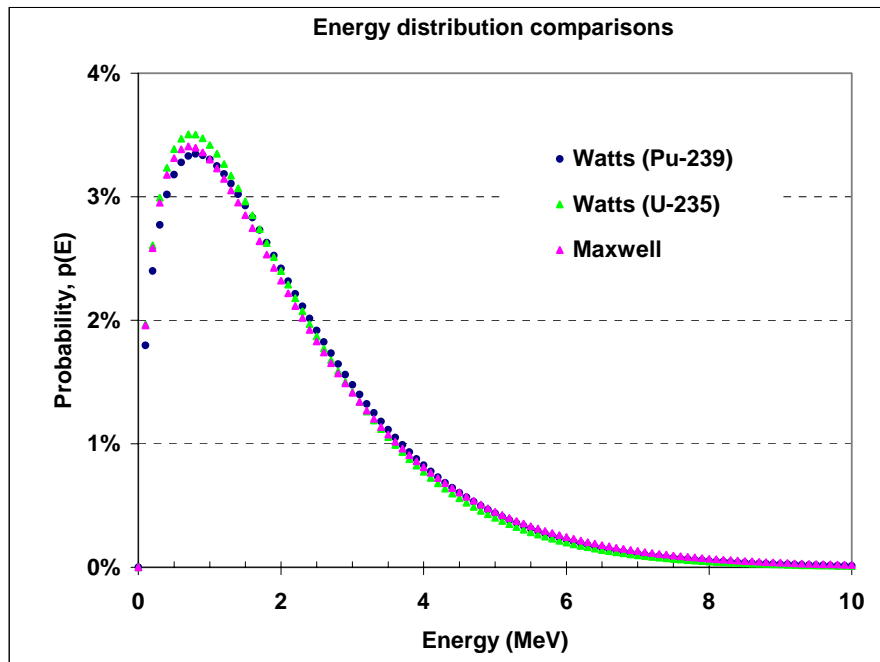
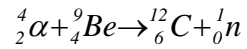


**Fig 1. Plot of Maxwell distribution equation compared to Watts distribution equations for U-235 and Pu-239.**

## Laboratory Neutron Source

Laboratory neutron sources are often made by combining a powdered  $\alpha$ -source, such as Pu-239, with a powdered light metal, such as Be, and encapsulating them in stainless steel. This becomes a “radiative” PuBe neutron source due to the following reaction:



While the neutrons are emitted with a continuous energy spectrum, the average neutron energy from a PuBe source is 4.5 MeV (Turner 1995).

A 1-Curie PuBe neutron source with 15.95 g of Pu-239 and a neutron fluence of  $1.27 \times 10^{-6} \text{ n s}^{-1}$  was used as the neutron source in this project. Since the true energy spectrum of neutrons emitted is unknown, Los Alamos National Laboratory generated an assumed spectrum (Figure 2) from the Sources-3A code (RSICC 2002), using known parameters and a common PuBe density of  $5 \text{ g/cm}^3$ .

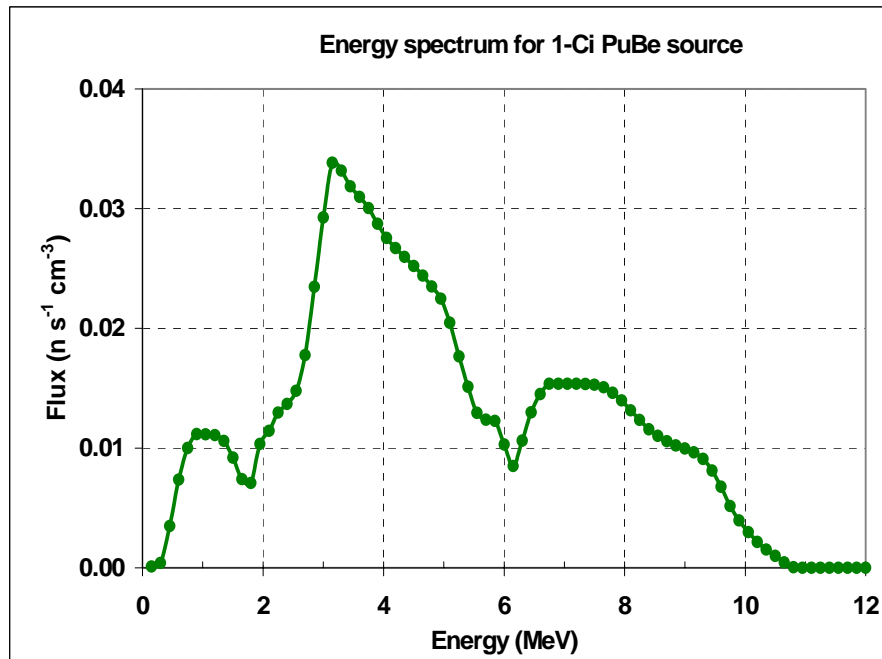


Fig 2. Calculated energy spectrum of neutrons from a 1-Ci PuBe source. Spectrum produced by Los Alamos National Laboratory using the Sources-3A code with assumed parameters of 16-g Pu-239 and density of 5 g/cc for the PuBe source.

### Cylindrical BF<sub>3</sub> Detectors

Two available cylindrical BF<sub>3</sub> detectors manufactured by LND, Inc. were used in this project to detect thermal neutrons. The LND 20210 BF<sub>3</sub> detector (gas volume = 111 cm<sup>3</sup>, pressure = 0.9 atm) was much more efficient than the LND 201 (gas volume = 6 cm<sup>3</sup>, pressure = 0.7 atm) due to its larger gas volume (LND 2002).

## **Evaluation of MCNP Functions Using Spherical $\text{BF}_3$**

The first objective was to evaluate various MCNP functions and understand MCNP capabilities and limitations as related to this project. To accomplish this, MCNP input files were created to model a 1-cm radius spherical detector containing  $\text{BF}_3$  gas at atmospheric pressure. Water shells of various thicknesses surrounded the detector. Neutron sources placed 50-cm from the center of that detector included a pencil beam such that the neutrons originated from a single point and traveled along a single vector toward the detector center; a plane parallel beam such that the neutrons originated from the surface of a plane and traveled parallel toward the detector center; and an isotropic point source such that the neutrons originated from a single point but produced a uniform fluence in all directions. These series used very simple geometries to evaluate the response of MCNP to controlled variables, even though none of these three sources would simulate the likely configuration of transported nuclear materials. MCNP response to modeled geometries was thereby evaluated by varying only one parameter at a time.

As discussed previously, hydrogen not only effectively moderates fast neutrons but it also competes with Boron to capture the neutrons once they become thermal. This problem was addressed by placing a carbon or lead shell between the detector and the moderator. Carbon and lead are chosen partly because they have essentially no probability of capturing neutrons and we therefore do not have the competition occurring with the  $\text{BF}_3$  as we do for hydrogen. Therefore, a 1-cm thick carbon shell or a lead shell was placed around the detector inside the water moderator to evaluate any changes in detector-measured counts.

## **Evaluation of Modeling Accuracy Using LND 201 BF<sub>3</sub>**

The second objective was to evaluate the accuracy of modeling, and resulting MCNP-generated data, based on data obtained from laboratory measurements. The LND 201 BF<sub>3</sub> detector includes a set of concentric cylindrical rings made of Lucite to moderate incident fast neutrons. Two-hour measurements were taken with the LND 201 for each Lucite moderator ring by placing the detector and 1-Ci PuBe source 1-m apart and at the same height in the laboratory. Appendix A shows the configuration of the PuBe source and BF<sub>3</sub>/moderator within the counting laboratory. Two-hour background measurements were also taken for each ring with the neutron source placed back in storage in the basement of the building.

The laboratory, the PuBe source, the detector, and the moderator(s) were then modeled in MCNP to include their dimensions, locations and compositions. Physical dimensions were measured and input into MCNP to model the counting laboratory. The walls and floor were modeled as concrete, the ceiling as CELOTEX fiberboard and the cabinets/counters as soft wood. The stand for the detector and moderators was not modeled because the four legs presented very low neutron scatter potential. The detector and moderator were thus considered “free floating”. Manufacturer data estimates the PuBe source strength as  $1.27 \times 10^6$  neutrons per second so that in a 2-hour counting interval,  $9.144 \times 10^9$  neutrons are emitted. MCNP generates the captures in the BF<sub>3</sub> per source neutron. To compare these results to those obtained from lab measurements, the MCNP results were multiplied by  $9.144 \times 10^9$  to give the number of captures in the BF<sub>3</sub> from neutrons emitted in a 2-hour interval.

Three series of runs were required to achieve acceptable accuracy when compared to the laboratory data. For the first series, the laboratory walls, ceiling, floor and counters were omitted to see if neutrons that might be scattered off them would influence the results. Any potential neutron scatter events were not included. Next, the floor, ceiling and far walls were modeled as closely as possible and the countertops on either side of the neutron source and detector were modeled as walls for simplicity. Contrary to the first series, if any neutron scatter occurred, it would be included. The final series was run with the countertops modeled very near their actual height (accounting for some variation where they held computers, other detectors, electronics, etc.). From this set of data, we intended to gain confidence that a given environment, source and detector could be modeled in MCNP such that it produced results very close to those measured in the laboratory.

The last series was repeated using a lead sleeve, and then a carbon sleeve, in place of one of the Lucite rings to evaluate the impact on captures. This was similar to the evaluation done in the spherical detector series.

### **Use of MCNP to Model Detection of Weapons-Grade Nuclear Material in Checked Baggage**

To demonstrate the feasibility of detecting Weapons-Grade Nuclear Material (WGNM) in a suitcase, MCNP was used to model a checked-baggage x-ray system similar to those in use at most airports. It was assumed that a small quantity of WGNM might be transported in a suitcase in or out of the country and that that suitcase would have to pass through an explosive detection system (EDS) employing x-rays. Internet

searches and discussions with manufacturers indicated that the InVision CTX 5500DS was a commonly used system to screen checked-baggage in the United States. Shown in Figures 3 and 4, it first acquires a fixed projection x-ray of a bag in the SP (scan projection) module and analyzes it to identify suspicious objects that require computed tomography (CT) slices in the next step. The bag then enters the CT module where an x-ray tube revolves to create CT slices that are analyzed by algorithms and matched against known weapons, explosives components, etc. Positive matches then sound alarms (InVision 2002).



**Fig 3. InVision CTX 5500DS EDS at Baltimore-Washington International (BWI) airport. [www.excite.com]**

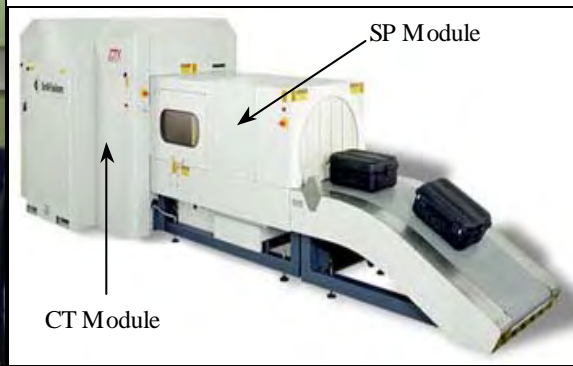


**Fig 4. InVision CTX 5500DS EDS for checked-baggage screening [www.invision-tech.com]**

While the x-ray system is intended to detect suspicious shapes,  $\text{BF}_3$  detectors could be placed inside the SP Module as well, above and below each bag, as it passes through on a conveyor. As such, MCNP runs were made for both the LND 201 and the LND 20210  $\text{BF}_3$  detectors. For example, one LND 201 was placed inside the SP Module above the suitcase and moderated by various thickness polyethylene cylinders while the other identical detector was placed inside the SP Module below the conveyor belt.

The WGNM and container were modeled as either a 100-g of Pu-239, WGP, U-235 or WGU (in the form of a 1-mm thick sheet to prevent criticality) surrounded by polyurethane foam inside a plastic suitcase. This suitcase then moved into the SP module that housed the two  $\text{BF}_3$  detectors and allowed a conveyor to pass through. Based on the known emission rate and energy spectrum of neutrons from the WGNM, calculations were made to determine if the detectors were efficient enough to detect neutrons at a rate that was at least ten times the normal background rate of neutrons. The background rate of neutrons was estimated from laboratory experiments.

Appendix B shows the configuration of the  $\text{BF}_3$  detectors, WGNM and suitcase inside the InVision CTX 5500DS as modeled in MCNP.

## RESULTS AND DISCUSSION

### Watts Thermal Neutron-Induced Fission Spectrum of Pu-239

A simple input file was written with an isotropic point source of Pu-239 emitting neutrons, due to induced fission, and placed inside a void. By tallying the energy of the neutrons that cross the surface of some sphere defining the void region, we compared the neutrons being emitted from the source to the input Watts energy spectrum equation. Since the source neutrons were emitted into a void and could therefore have no interactions, the neutrons crossing the sphere surface have the same energy distribution as the source neutrons. The resulting Watts fission spectrum is shown in Fig 5.

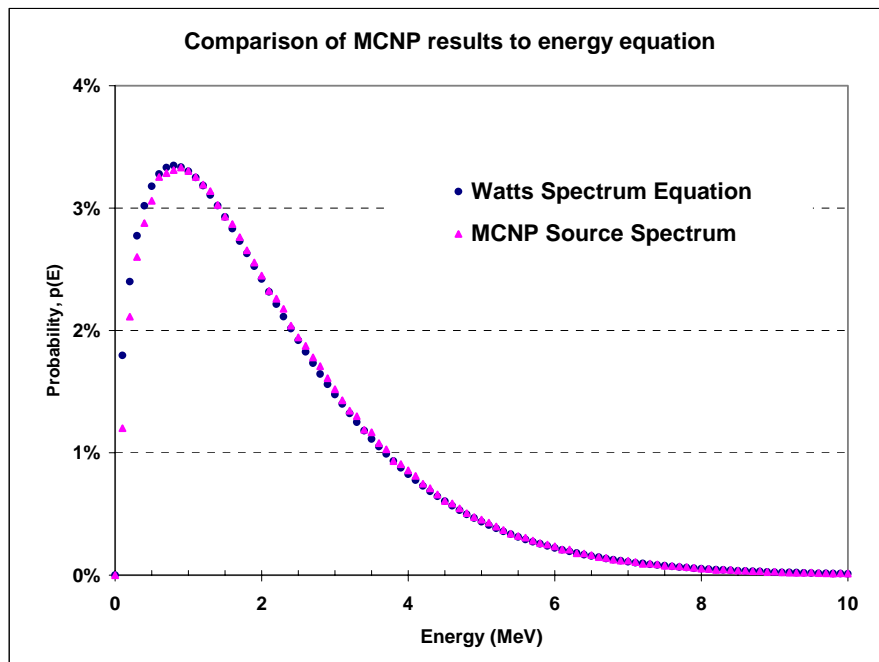


Fig 5. Comparison of MCNP results for energy of source neutrons to plot of Watts energy spectrum equation.

## **Evaluation of MCNP Functions Using Spherical $\text{BF}_3$**

### Pencil Beam Neutron Source

Source neutrons from a pencil beam were specified to be either mono-energetic (0.5, 1, or 2 MeV each) or to have a Watts energy distribution. They were then emitted from a common point along a common vector toward the center of the detector. Water was added in spherical shells around the  $\text{BF}_3$  to act as a moderator.

Figure 6 shows the measured counts of the  $\text{BF}_3$  detector inside water to neutrons from a pencil beam. As expected, the number of captures in the  $\text{BF}_3$  decreases as the moderator size increases because while the water efficiently slows the source neutrons, it also captures them after sufficient moderation. Hydrogenated materials, therefore, pose a dilemma in that they are very effective at slowing the neutrons enough for captures to occur in the  $\text{BF}_3$  as desired, yet hydrogen also competes for the capture of those slowed neutrons with the  $\text{BF}_3$ .

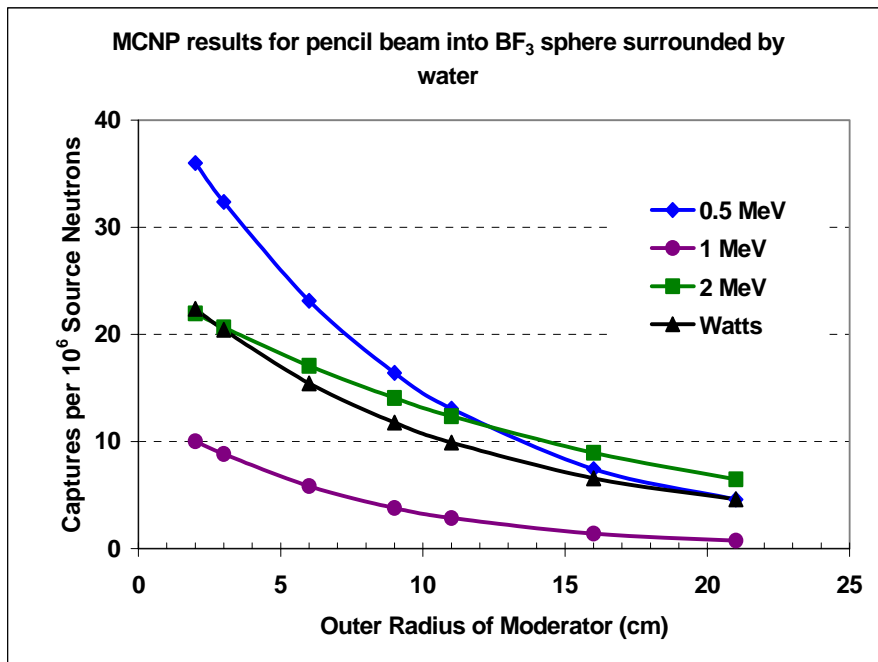


**Fig 6.** MCNP results for captures in 1-cm radius  $\text{BF}_3$  sphere.  $\text{BF}_3$  was surrounded by water and was exposed to neutrons with various energies from a pencil beam source.

As previously stated, one must maximize the captures which occur in the  $\text{BF}_3$  relative to captures occurring elsewhere in the detector environment. Figure 7 shows that for neutrons from a pencil beam into a water-moderated detector, essentially all of the captures occur in the water with very few in the  $\text{BF}_3$  or in the air surrounding the detector system.

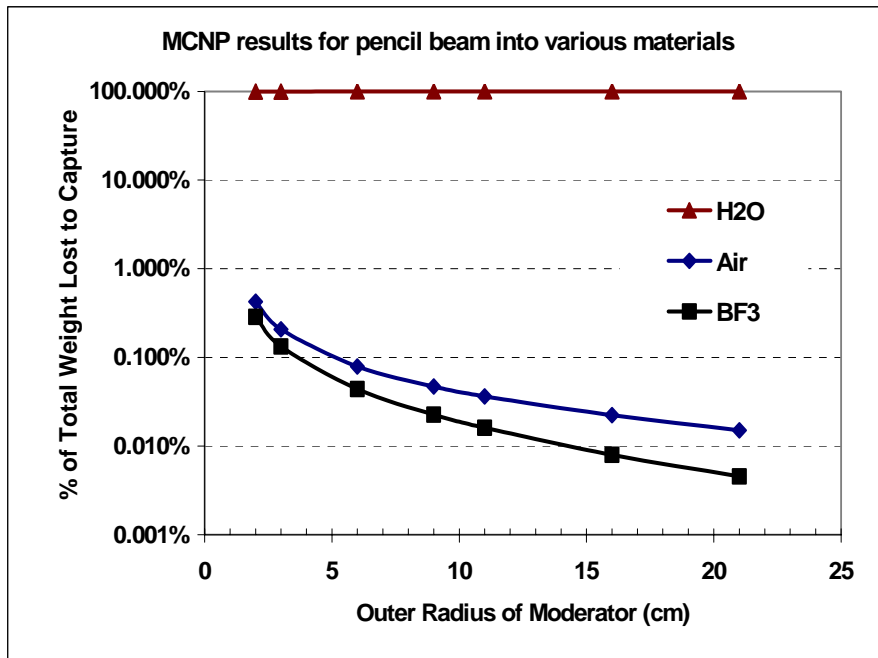
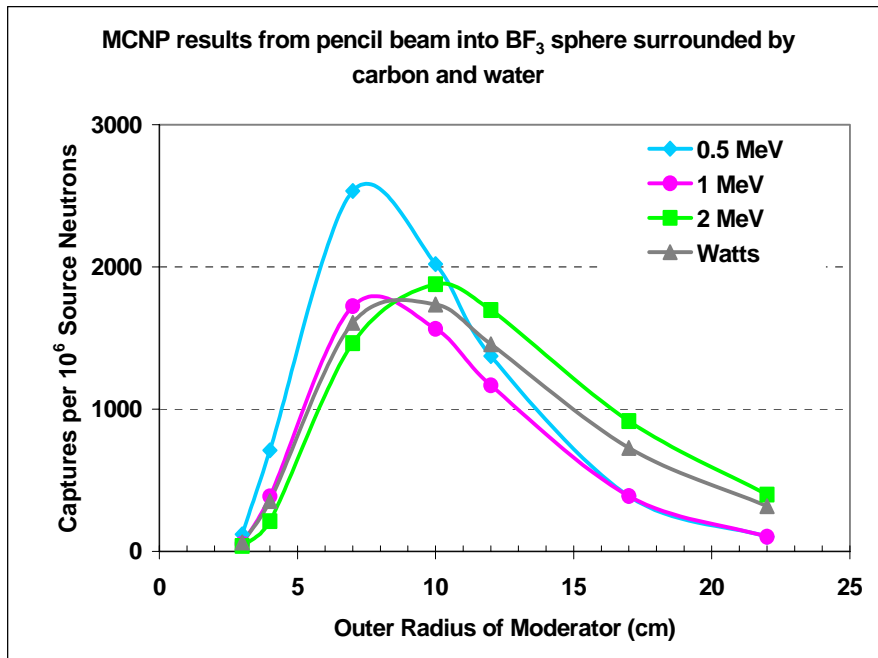


Fig 7. MCNP results for percent of all captures in 1-cm radius  $\text{BF}_3$  sphere, water, or in air from Watts pencil beam neutrons.

Since captures in the water are dominating captures in the  $\text{BF}_3$ , 1-cm thick carbon was added around the detector in an attempt to increase the captures in the  $\text{BF}_3$ . Figure 8 shows the results for this geometry where the maximum captures occur at a total radius of 7-10 cm. At smaller radii, the source neutrons are not yet sufficiently moderated to be captured in the  $\text{BF}_3$ , while at higher radii captures in the water moderator dominate.

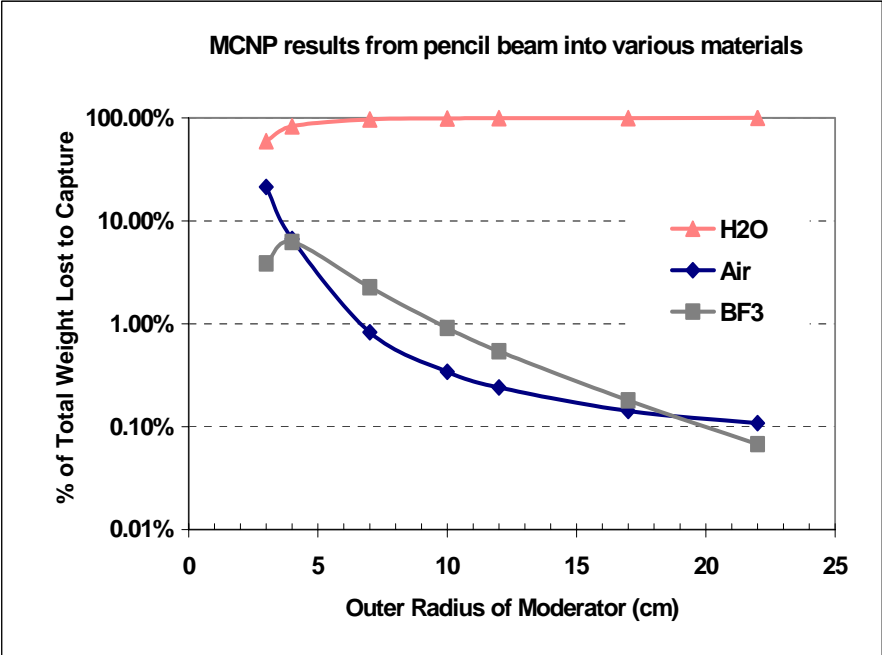


**Fig 8. MCNP results for captures in 1-cm radius  $\text{BF}_3$  sphere.  $\text{BF}_3$  was surrounded by water and carbon and was exposed to neutrons with various energies from a pencil beam source.**

Figures 6 and 8 also illustrate that the Watts spectrum neutron source result is similar to an average of the 0.5, 1 and 2 MeV monoenergetic neutron source results. Therefore, all remaining results for the spherical  $\text{BF}_3$  detector will be for Watts spectrum neutrons only.

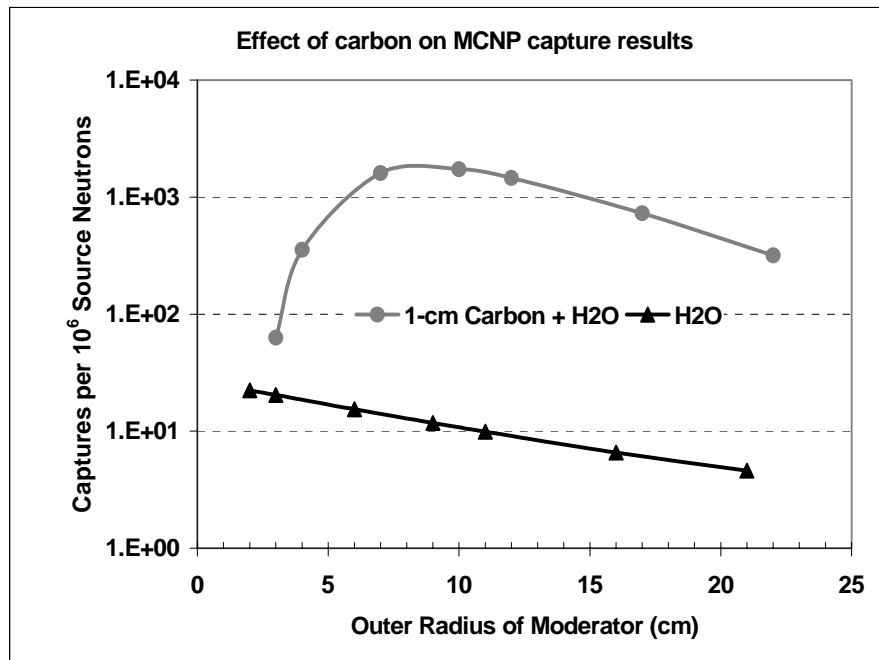
Captures occur in all materials in the problem but at different probabilities.

Figure 9 shows the distribution of captures among the air (surrounding moderator and source), water and  $\text{BF}_3$  for pencil beam neutrons into water and a 1-cm thick carbon shell. Most of the captures still occur in the water.



**Fig 9. MCNP results for percent of all captures in 1-cm radius  $\text{BF}_3$  sphere, 1-cm thick carbon, water, or in air from Watts pencil beam neutrons.**

Figure 10 compares the results of a pencil beam source of neutrons incident on a  $\text{BF}_3$  detector surrounded by water only to one surrounded by water and 1-cm thick carbon.



**Fig 10.** Comparison of MCNP results for captures in 1-cm radius  $\text{BF}_3$  sphere.  $\text{BF}_3$  was surrounded by water, or by water and carbon, and was exposed to neutrons with Watts spectrum energies from a pencil beam source.

As hypothesized, including the carbon shell increases the lifetime of a neutron reaching it as evidenced by the significantly higher Mean Time to Capture in Figure 11 for the carbon series versus the water only series. Mean Time to Capture is defined as the average time, in shakes (shake =  $10^{-8}$  sec), from when a neutron is emitted from the source until the time that it is captured in some medium.

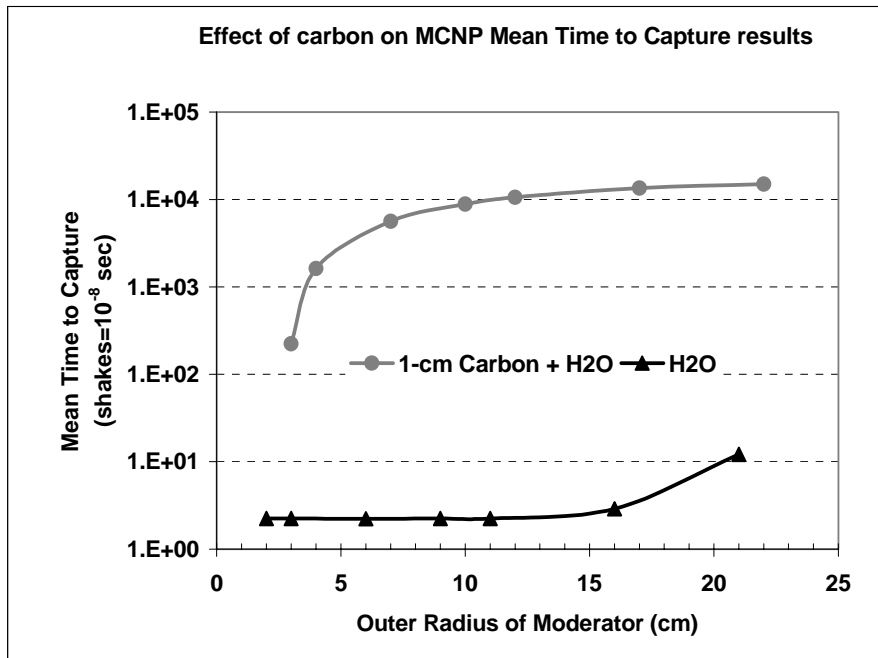
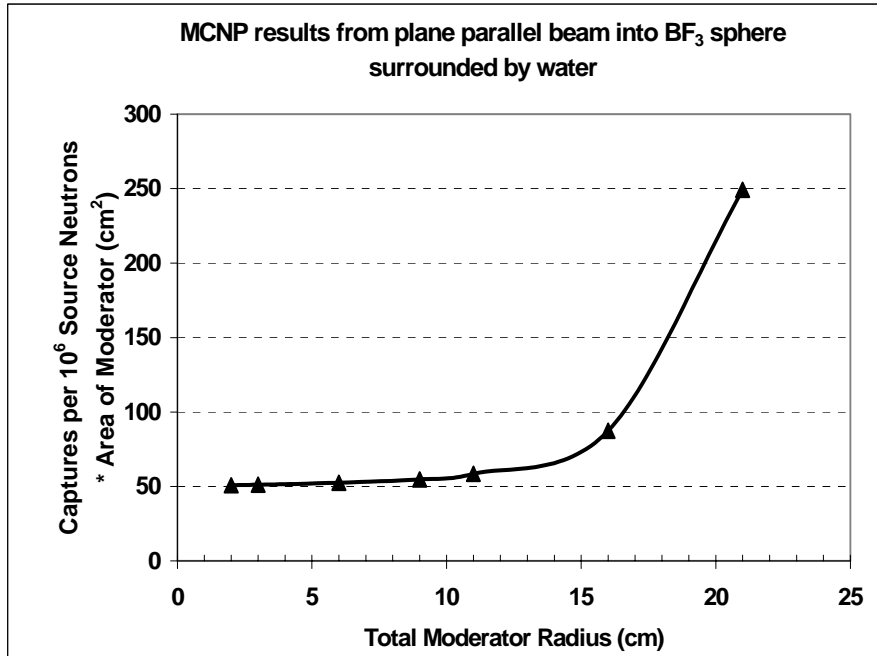


Fig 11. Comparison of MCNP results for Mean Time to Capture in any material.  $\text{BF}_3$  was surrounded by water, or by water and carbon, and was exposed to neutrons with Watts spectrum energies from a pencil beam source.

## Plane Parallel Beam Neutron Source

Figure 12 shows the number of captures occurring in the  $\text{BF}_3$  sphere as a function of increasing moderator size. As opposed to the measured counts to a pencil beam neutron source, plane parallel beam neutron captures increase as the moderator thickness increases. The source neutrons are emitted from a circular plane of equal radius to the cross-section of the water moderator. The MCNP data was multiplied by the area of the source circle in order to normalize the results to the same neutron fluence.



**Fig 12. MCNP results for captures in 1-cm radius  $\text{BF}_3$  sphere.  $\text{BF}_3$  was surrounded by water and was exposed to neutrons with Watts spectrum energies from a plane parallel beam source.**

Figure 13 shows that, for neutrons from a plane parallel beam into a water-moderated detector, the water accounts for essentially all of the captures.

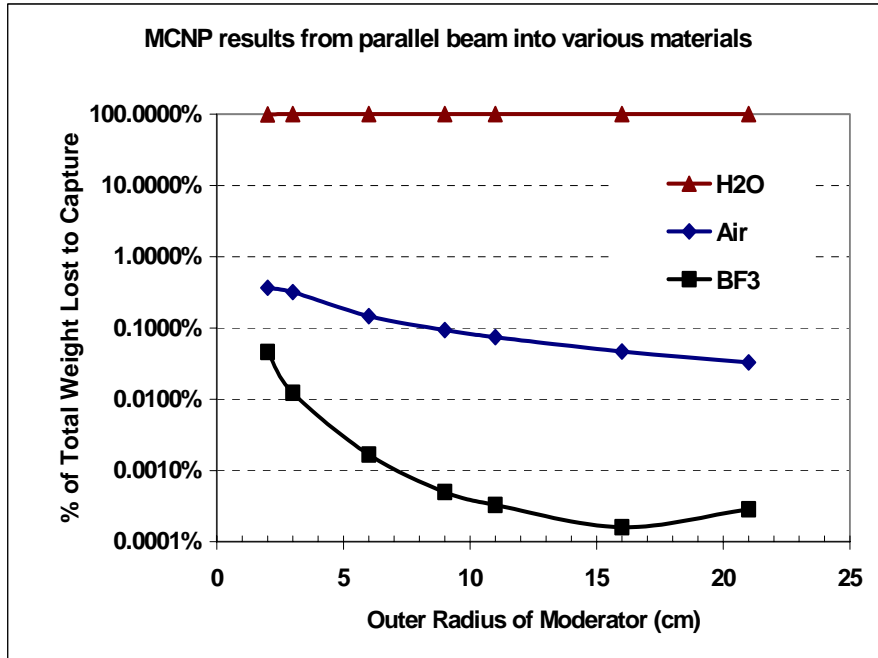
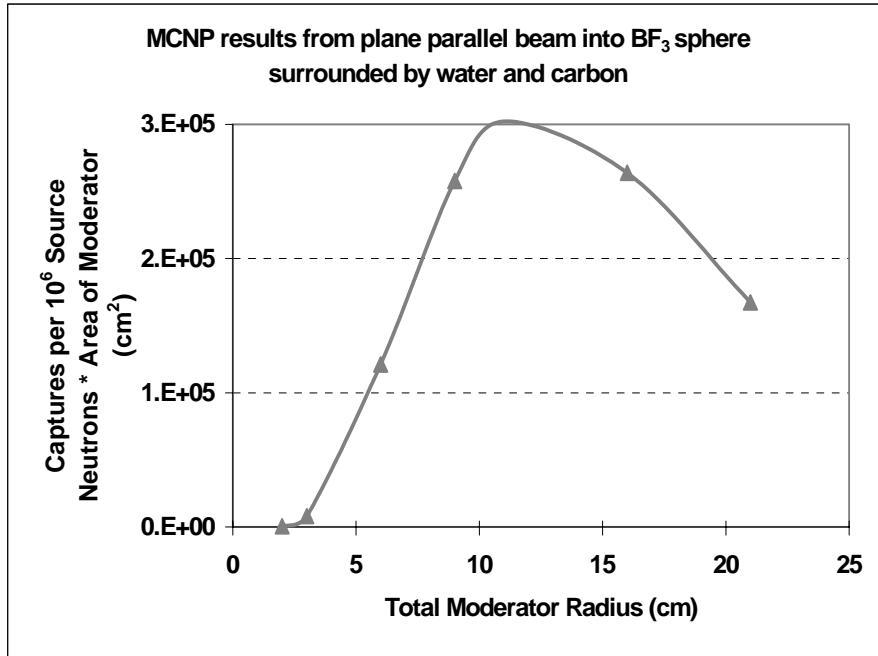


Fig 13. MCNP results for percent of all captures in 1-cm radius  $\text{BF}_3$  sphere, water, or in air from Watts plane parallel beam neutrons.

Figure 14 shows the normalized captures in  $\text{BF}_3$  when it is surrounded by 1-cm thick carbon and various thickness water shells.



**Fig 14.** MCNP results for captures in 1-cm radius  $\text{BF}_3$  sphere.  $\text{BF}_3$  was surrounded by water and carbon and was exposed to neutrons with Watts spectrum energies from a plane parallel beam source.

Figure 15 shows the distribution of captures among the air (surrounding moderator and source), water and BF<sub>3</sub> for plane parallel beam neutrons into water and a 1-cm thick carbon shell. Water still is the predominant medium in which captures occur.

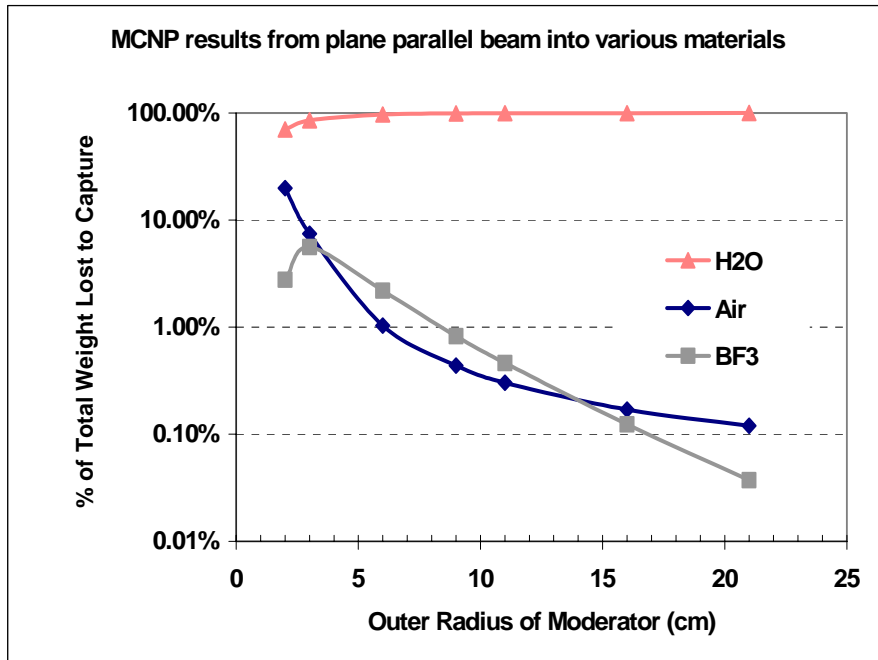


Fig 15. MCNP results for percent of all captures in 1-cm radius BF<sub>3</sub> sphere, 1-cm thick carbon, water, or in air from Watts plane parallel beam neutrons.

Figure 16 compares the results of a plane parallel beam source of neutrons incident on a  $\text{BF}_3$  detector surrounded by water only to one surrounded by water and 1-cm thick carbon.

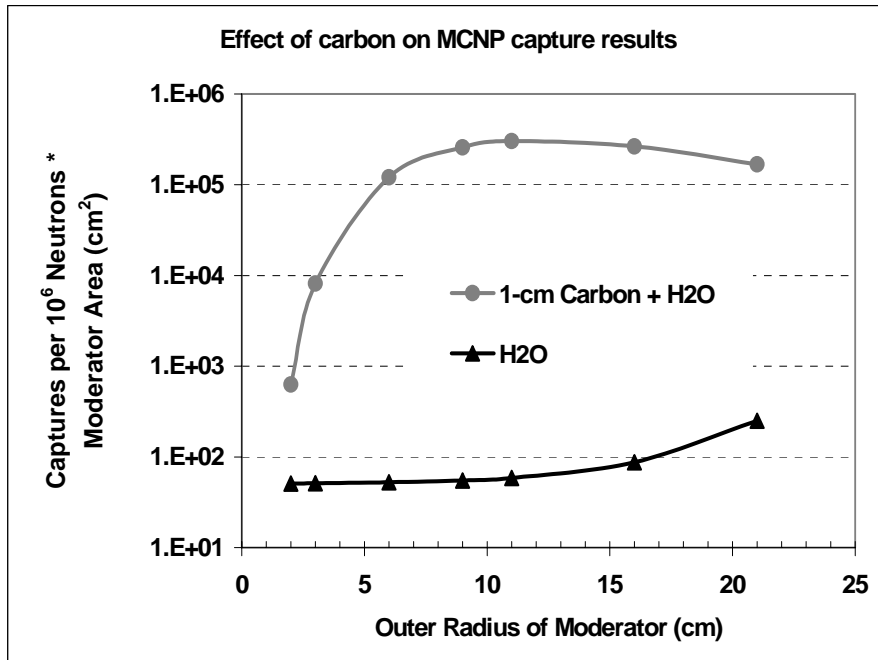


Fig 16. Comparison of MCNP results for captures in 1-cm radius  $\text{BF}_3$  sphere.  $\text{BF}_3$  was surrounded by water, or by water and carbon, and was exposed to neutrons with Watts spectrum energies from a plane parallel beam source.

As hypothesized, including the carbon shell increases the lifetime of a neutron reaching it as evidenced by the significantly higher Mean Time to Capture in Figure 17 for the carbon series versus the water only series. Mean Time to Capture is defined as the average time, in shakes, from when a neutron is emitted from the source until the time that it is captured in some medium.

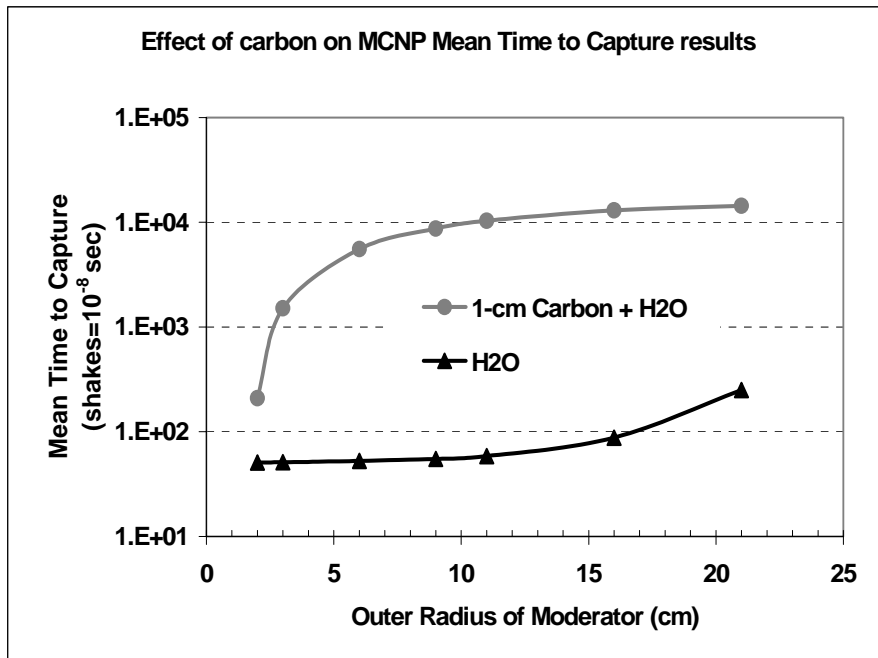
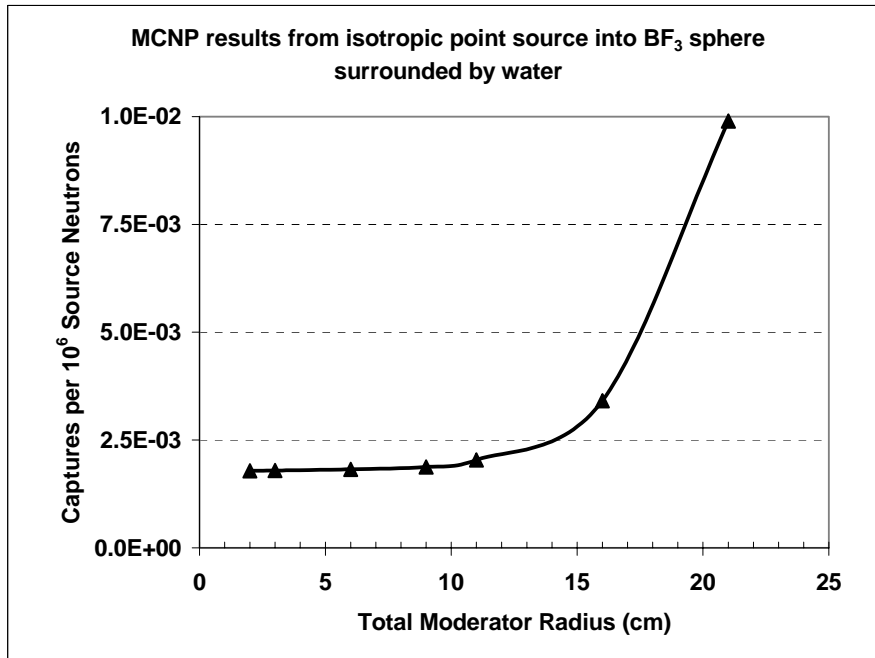


Fig 17. Comparison of MCNP results for Mean Time to Capture in any material.  $\text{BF}_3$  was surrounded by water, or by water and carbon, and was exposed to neutrons with Watts spectrum energies from a plane parallel beam source.

## Isotropic Point Neutron Source

Figure 18 shows that the number of captures occurring in the spherical  $\text{BF}_3$  increase as the moderator thickness increases. The shape of the measured counts is identical to the normalized measured counts of the detector when exposed to plane parallel beam neutrons. This results because at a source to detector distance of 50-cm, the neutrons that reach the moderator are essentially parallel to each other and thereby appear to the detector like a smaller and weaker plane parallel beam source.



**Fig 18. MCNP results for captures in 1-cm radius  $\text{BF}_3$  sphere.  $\text{BF}_3$  was surrounded by water and was exposed to neutrons with Watts spectrum energies from an isotropic point source.**

Figure 19 shows that, for neutrons from a isotropic point into a water-moderated detector, the water accounts for essentially all of the captures above  $r = 8$  cm. Below  $r = 8$  cm, air captures a significant portion of those neutrons which interact in the moderator and subsequently escape into the surrounding air.

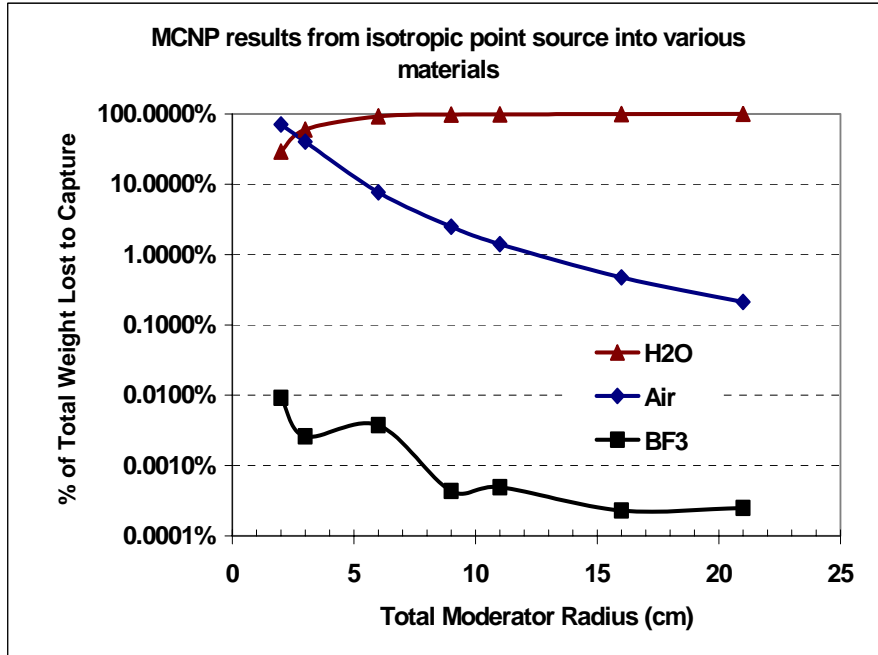
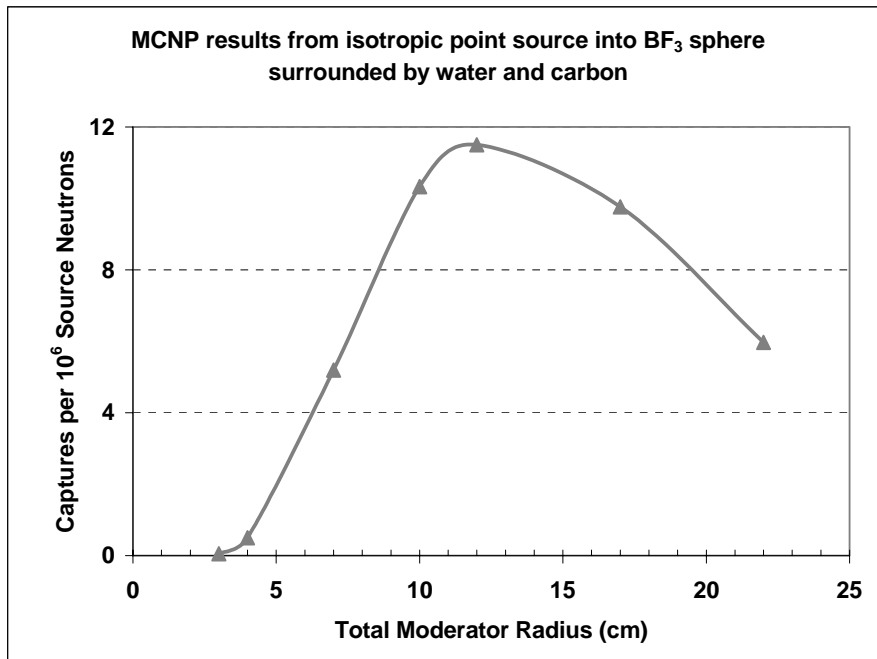


Fig 19. MCNP results for percent of all captures in 1-cm radius  $\text{BF}_3$  sphere, water, or in air from Watts isotropic point neutrons.

Figure 20 shows the captures occurring in the  $\text{BF}_3$  when the detector is surrounded by 1-cm thick carbon and varying thickness water shells. Again the shape of the measured counts is the same as the normalized results for a plane parallel beam source.



**Fig 20. MCNP results for captures in 1-cm radius  $\text{BF}_3$  sphere.  $\text{BF}_3$  was surrounded by water and carbon and was exposed to neutrons with Watts spectrum energies from an isotropic point source.**

Figure 21 shows the distribution of captures among the air (surrounding moderator and source), water and BF<sub>3</sub> for isotropic point source neutrons into water and a 1-cm thick carbon shell. Water still is the predominant medium in which captures occur although the captures in air after moderation cannot be ignored. Captures in the BF<sub>3</sub> reach a maximum at r=7 cm yet still only account for 1% of the total captures. Captures are most prevalent in the air after some moderation when r<7 cm and are most prevalent in water when r>7 cm.

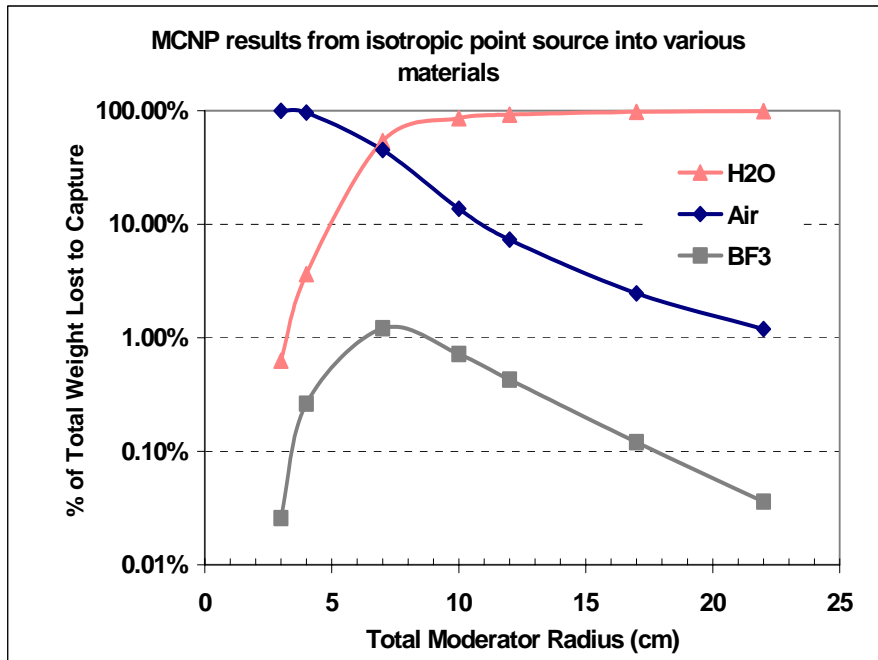


Fig 21. MCNP results for percent of all captures in 1-cm radius BF<sub>3</sub> sphere, 1-cm thick carbon, water, or in air from Watts isotropic point neutrons.

Figure 22 compares the results of an isotropic point source of neutrons incident on a  $\text{BF}_3$  detector surrounded by water only to one surrounded by water and 1-cm thick carbon.

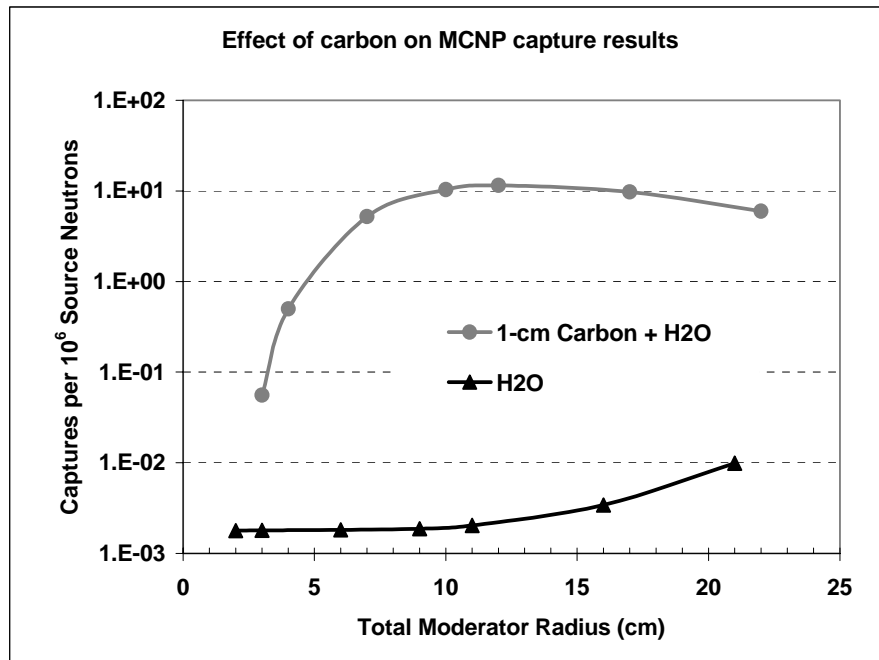


Fig 22. Comparison of MCNP results for captures in 1-cm radius  $\text{BF}_3$  sphere.  $\text{BF}_3$  was surrounded by water, or by water and carbon, and was exposed to neutrons with Watts spectrum energies from an isotropic point source.

As hypothesized, including the carbon shell increases the lifetime of a neutron reaching it as evidenced by the significantly higher Mean Time to Capture in Figure 23 for the carbon series versus the water only series. Mean Time to Capture is defined as the average time, in shakes, from when a neutron is emitted from the source until the time that it is captured in some medium.

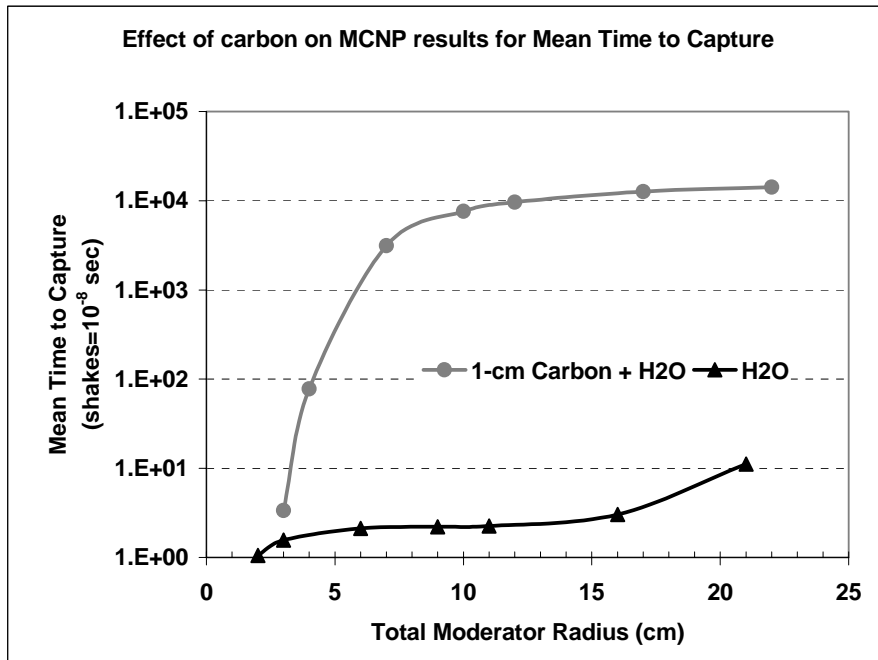


Fig 23. Comparison of MCNP results for Mean Time to Capture in 1-cm radius  $\text{BF}_3$  sphere.  $\text{BF}_3$  was surrounded by water, or by water and carbon, and was exposed to neutrons with Watts spectrum energies from an isotropic point source.

## Validation of MCNP Accuracy Using LND 201 BF<sub>3</sub>

### Lucite Moderator

Figure 24 shows typical gross counts from the lab measurements when the LND 201 is exposed to the 1-Ci PuBe source.

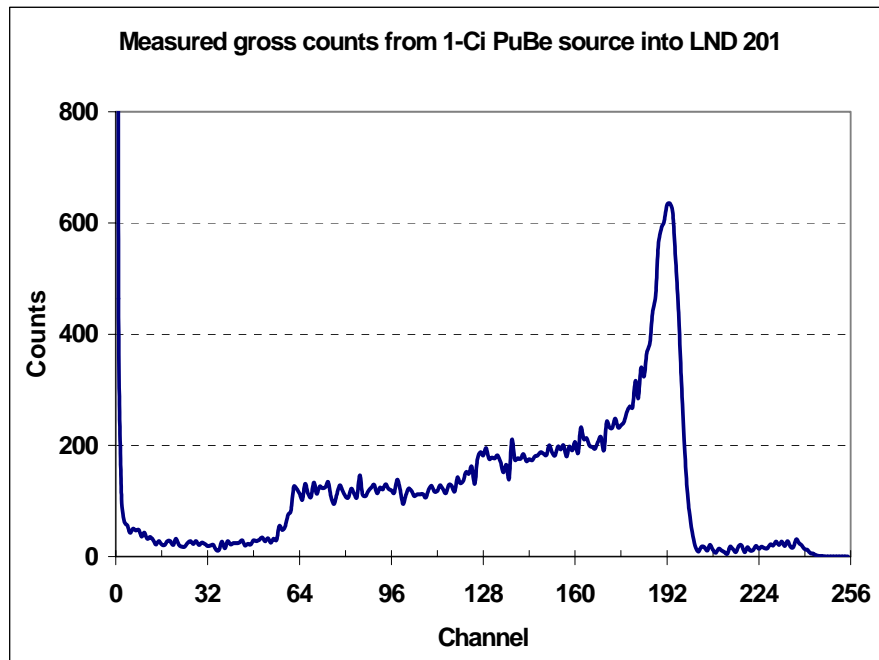


Fig 24. Lab results for gross counts in LND 201 moderated by Lucite ring 14 ( $r=8.95$  cm) when exposed to 1-Ci PuBe source for 2 hours at 1 m.

Figure 25 shows the cumulative percentage of the gross counts as a function of channel number.

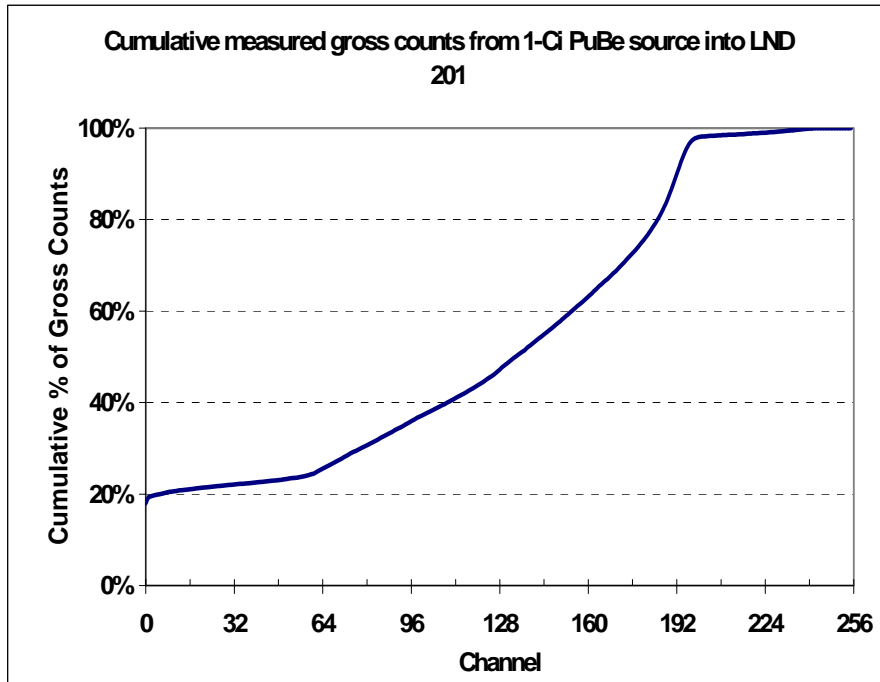
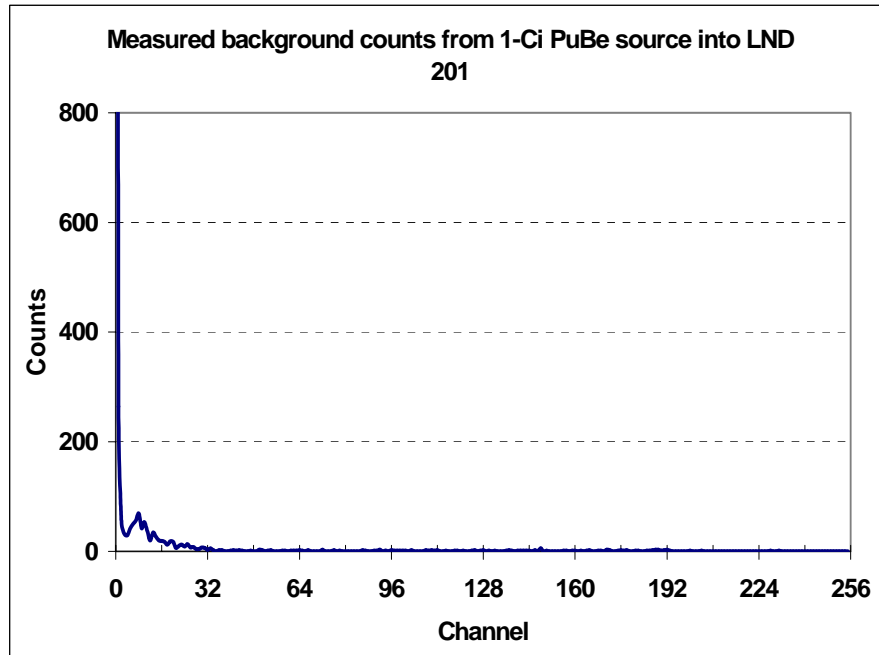


Fig 25. Cumulative lab results for gross counts in LND 201 moderated by Lucite ring 14 ( $r=8.95$  cm) when exposed to 1-Ci PuBe source for 2 hrs at 1 m.

After examining all measured counts spectra from the lab measurements, background noise (gamma and electronic) is seen mainly in Channels 0-31 (Figure 26) and these counts can be excluded by choosing a region of interest including Channels 32-255.



**Fig 26. Lab results for background counts in LND 201 moderated by Lucite ring 14 ( $r=8.95$  cm) when exposed to 1-Ci PuBe source for 2 hours at 1 m.**

Figure 27 shows that 98% of the background counts were measured within Channels 0-32. This supports selecting a discriminator at Channel 32 to eliminate background counts presumably due to  $\gamma$  radiation.

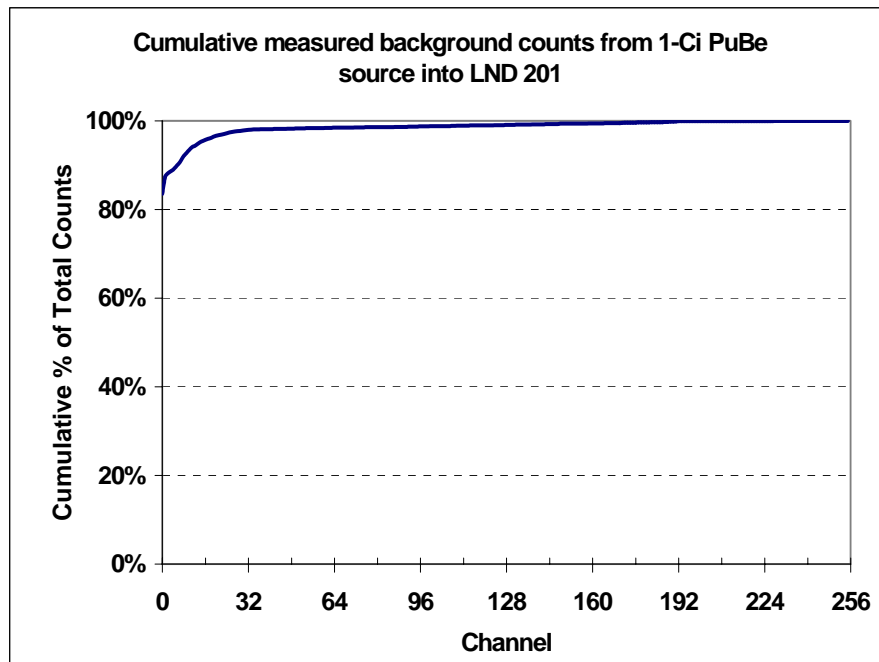


**Fig 27. Cumulative lab results for background counts in LND 201 moderated by Lucite ring 14 ( $r=8.95$  cm) when exposed to 1-Ci PuBe source for 2 hrs at 1 m.**

Figure 28 shows that selecting a discriminator at Channel 32 sacrifices few neutron counts that could have been included otherwise.

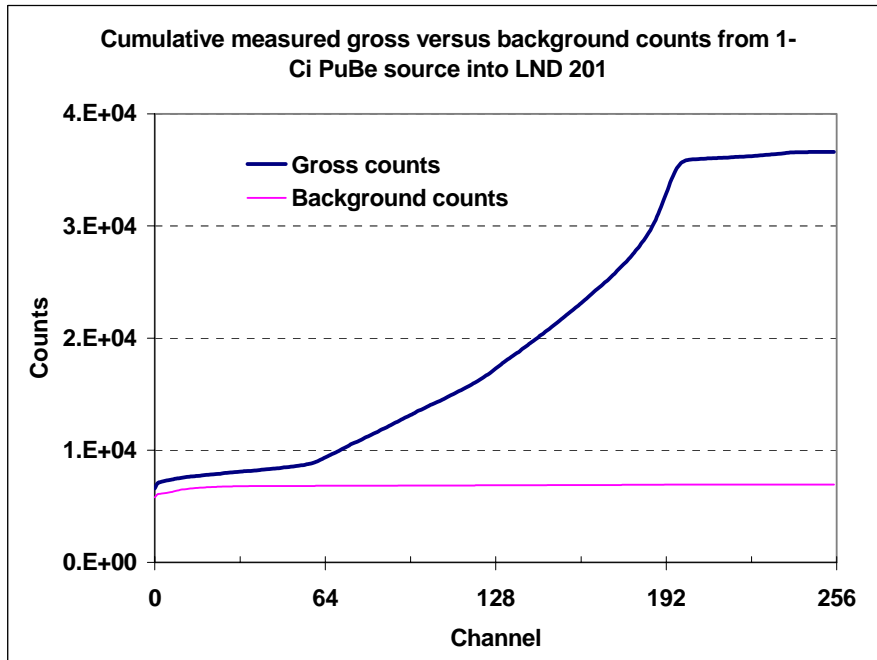


Fig 28. Cumulative lab results for gross versus background counts in LND 201 moderated by Lucite ( $r=8.95$  cm) when exposed to 1-Ci PuBe source for 2 hrs at 1 m.

Figure 29 shows the effect of including scatter in the MCNP modeling. The counting laboratory was first modeled without walls, ceiling, floor or counters. This served to eliminate neutron scatter and thereby underestimated the results obtained in the laboratory. Next, walls, floor and ceiling were included but the counters were modeled as walls rather than at their actual height. This served to add too much neutron scatter and thereby overestimated the laboratory data.

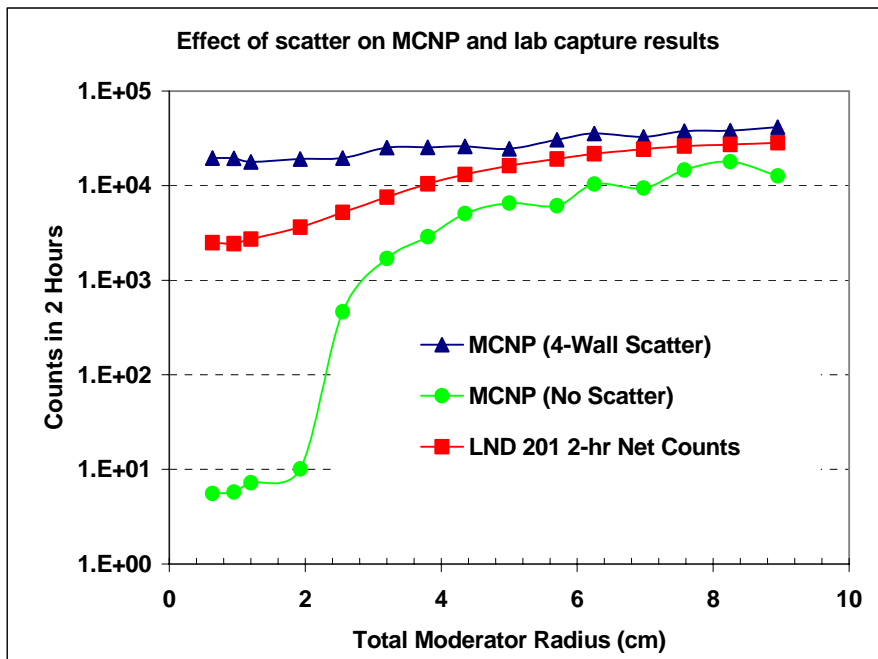


Fig 29. Comparison of MCNP results and lab results for captures in LND 201  $\text{BF}_3$  when scatter is either overestimated or underestimated.  $\text{BF}_3$  was surrounded by Lucite rings and was exposed to neutrons with Sources-3A spectrum energies from a PuBe source.

Figure 30 illustrates the excellent agreement of the MCNP results with the laboratory data when the counter heights were modeled, as they exist. The MCNP results were considered an accurate representation of the laboratory conditions using necessary assumptions with regards to compositions of materials in the room and how to model odd-shaped objects.

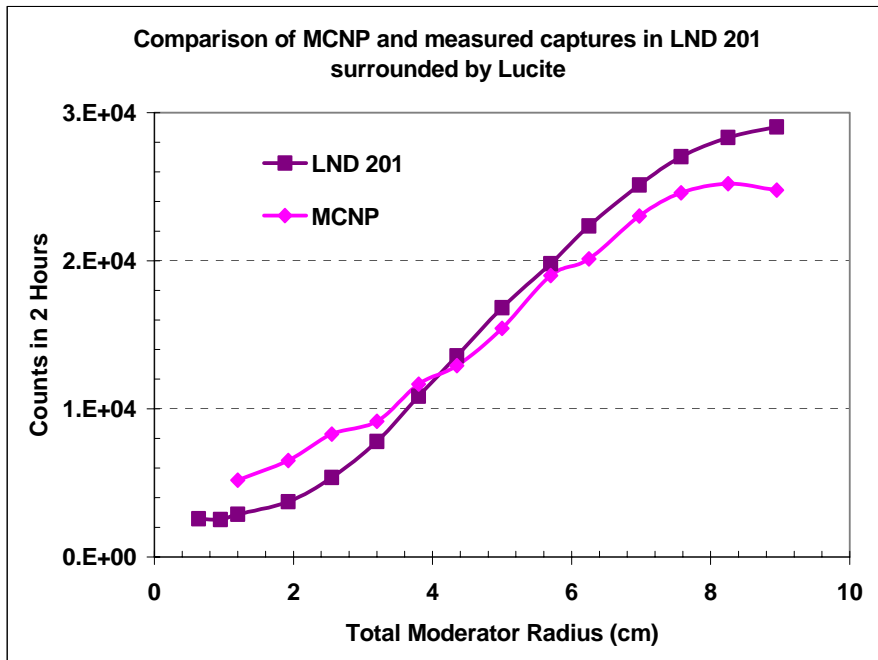
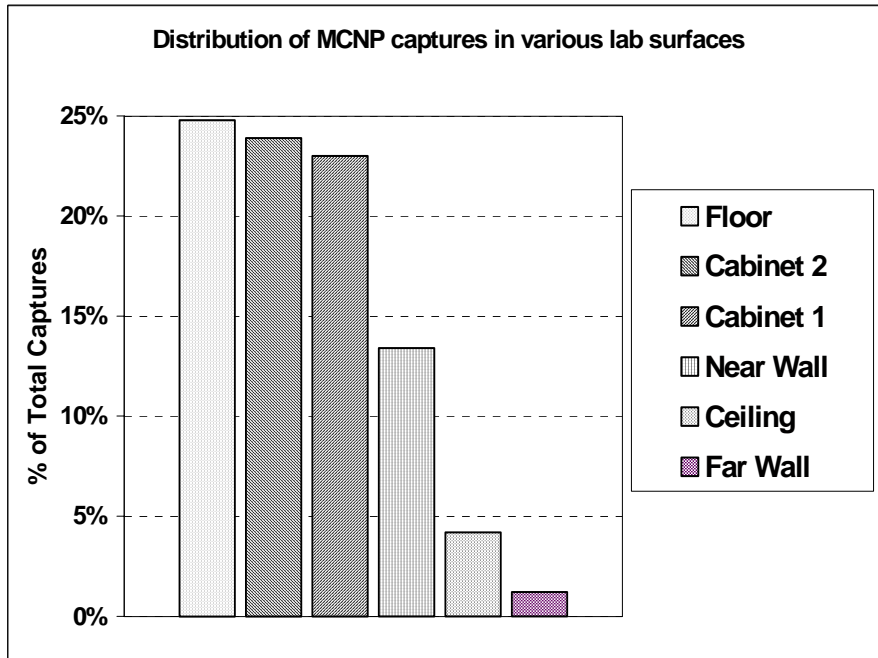


Fig 30. Comparison of MCNP results and lab results for captures in LND 201  $\text{BF}_3$  when scatter is correctly considered.  $\text{BF}_3$  was surrounded by Lucite rings and was exposed to neutrons with Sources-3A spectrum energies from a PuBe source.

Figure 31 shows that of the neutron captures that occur, most (90.5%) occur in the room surfaces rather than in the air, moderators, or BF<sub>3</sub> volume. This reemphasizes the importance of modeling accurately.



**Fig 31. MCNP results for distribution of captures in various lab surfaces from S-3A PuBe neutrons.**

## Lucite and Lead or Carbon Moderator

Another set of runs were made in the lab and in MCNP where Lucite Sleeve 3 (outer radius = 1.925 cm) was replaced with an equally thick lead cylinder in the hope that it would improve detector measured counts like it did in the spherical detector. Figure 32 shows the MCNP results compared to the laboratory data. The agreement of the two curves supports that the MCNP input parameters adequately represent the physical laboratory conditions.

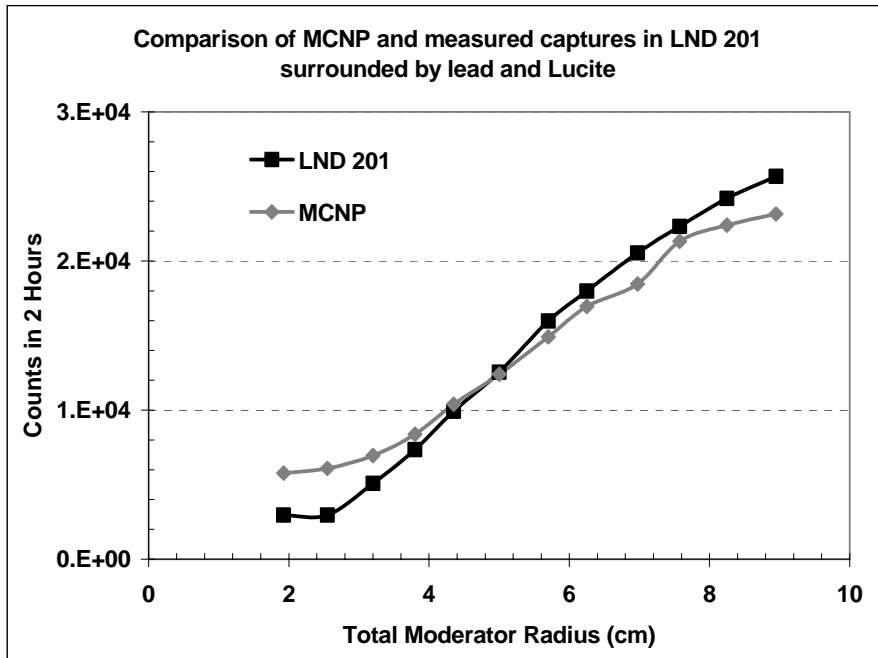
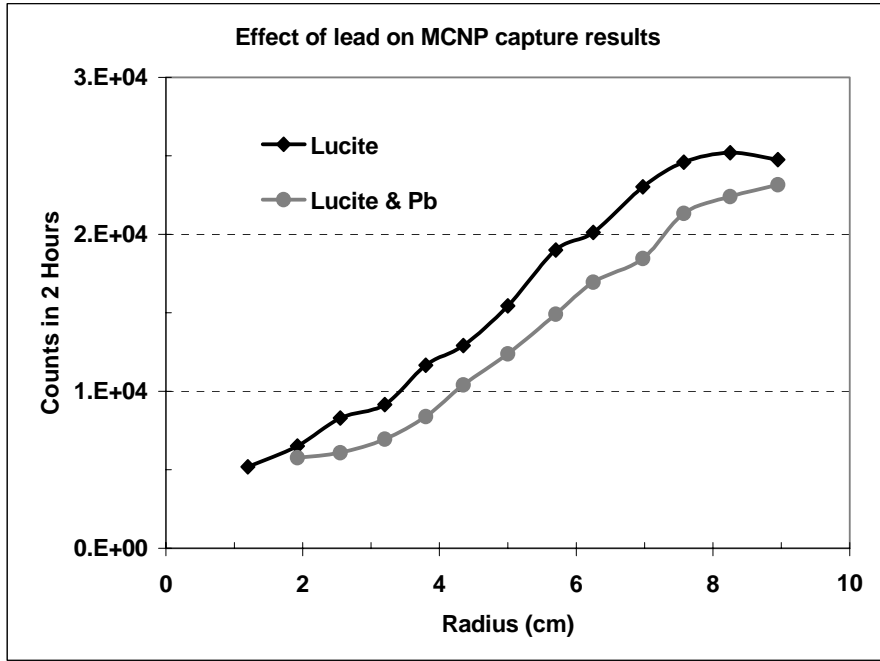


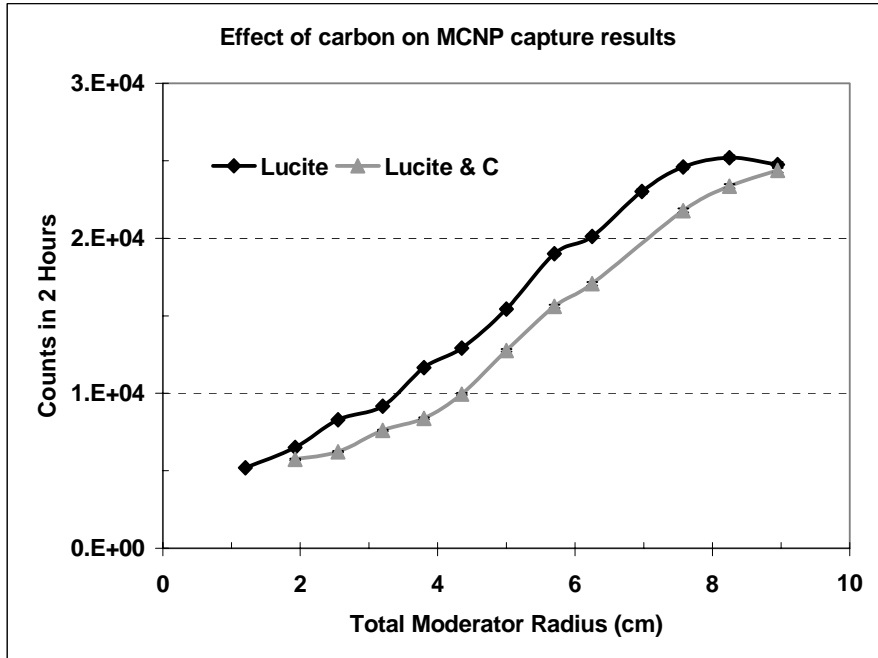
Fig 32. Comparison of MCNP results and lab results for captures in LND 201  $\text{BF}_3$ .  $\text{BF}_3$  was surrounded by lead sleeve and Lucite rings and was exposed to neutrons with Sources-3A spectrum energies from a PuBe source.

Figure 33 shows that using the lead sleeve in place of Lucite Sleeve 3 degraded the measured counts of the detector.



**Fig 33. Comparison of MCNP results for captures in LND 201. The  $\text{BF}_3$  was surrounded by either Lucite alone or by a lead sleeve and Lucite and exposed to neutrons with Sources-3A spectrum energies from a PuBe source.**

Similar to Figure 33, Figure 34 illustrates that replacing Sleeve 3 with carbon decreased detector measured counts when compared to Lucite moderation only.



**Fig 34. Comparison of MCNP results for captures in LND 201. The  $\text{BF}_3$  was surrounded by either Lucite alone or by a carbon sleeve and Lucite and exposed to neutrons with Sources-3A spectrum energies from a PuBe source.**

## Use of MCNP to Model Detection of Weapons-Grade Nuclear Material in Checked Baggage

Figure 35 shows the results of two LND 201s being exposed to a suitcase containing 100-g of weapons-grade nuclear material (WGNM). Four sets of results were collected for each WGNM studied: Pu-239, WGP, U-235 and WGU. Figure 35 is representative of the results of each of them. As modeled in MCNP, the LND 201s were exposed to a source originally emitting  $10^6$  neutrons with energies corresponding to a Watts distribution. The MCNP results for captures in the LND 201s are therefore independent of the source WGNM or the corresponding source strength. The results will be adjusted for these factors in a following table.

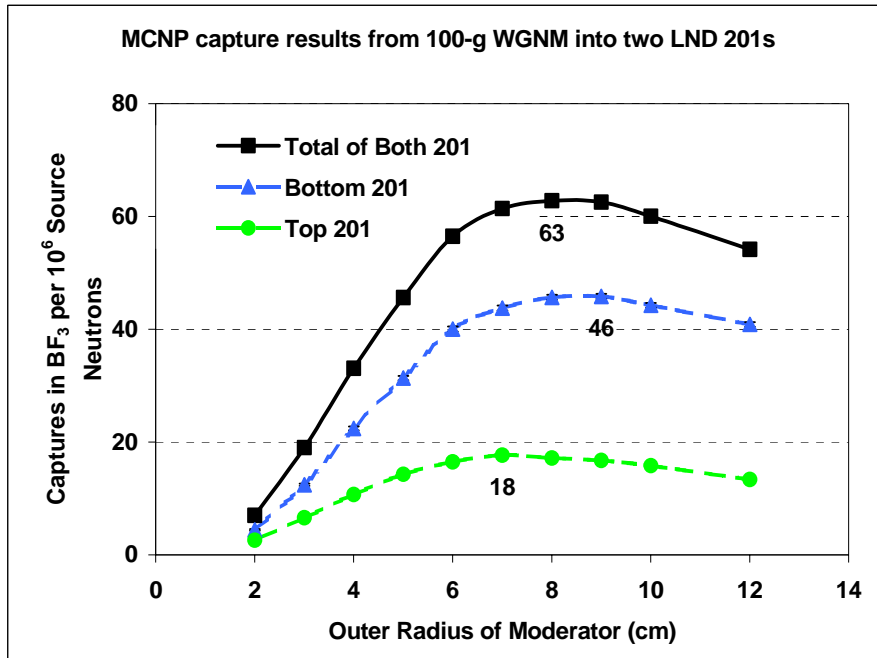
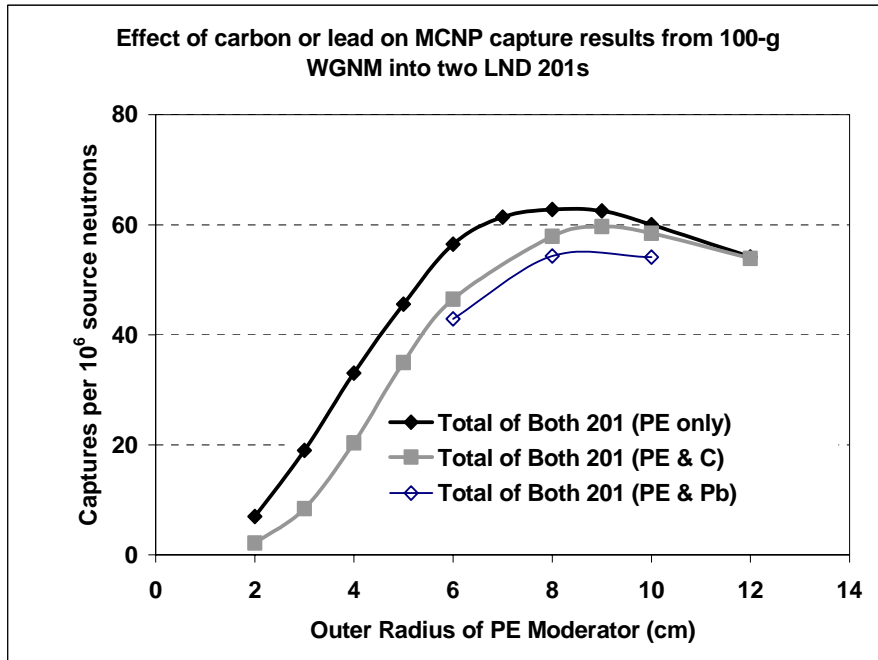


Fig 35. MCNP results for captures in LND 201s located above and below a suitcase. The  $\text{BF}_3$ s were moderated by polyethylene and exposed inside a CTX 5500 to the suitcase containing a 100-g, 1-mm thick sheet of WGNM.

Figure 36 shows the results of including 1-cm of carbon or lead around the  $\text{BF}_3$  detectors in an attempt to increase measured counts. As seen in previous modeling of the cylindrical  $\text{BF}_3$  detectors, lead or carbon decreased measured counts.



**Fig 36.** Comparison of MCNP results for captures in LND 201s located above and below a suitcase. The  $\text{BF}_3$ s were moderated by polyethylene alone or by polyethylene/carbon or polyethylene/lead. The  $\text{BF}_3$ s were exposed inside a CTX 5500 to the suitcase containing a 100-g, 1-mm thick sheet of WGM.

Figure 37 shows the results of two LND 20210s being exposed to a suitcase containing 100-g of weapons-grade nuclear material (WGNM). As with the LND 201s, four sets of results were collected for each WGNM studied: Pu-239, WGP, U-235 and WGU. Figure 35 is representative of the results of each of them.

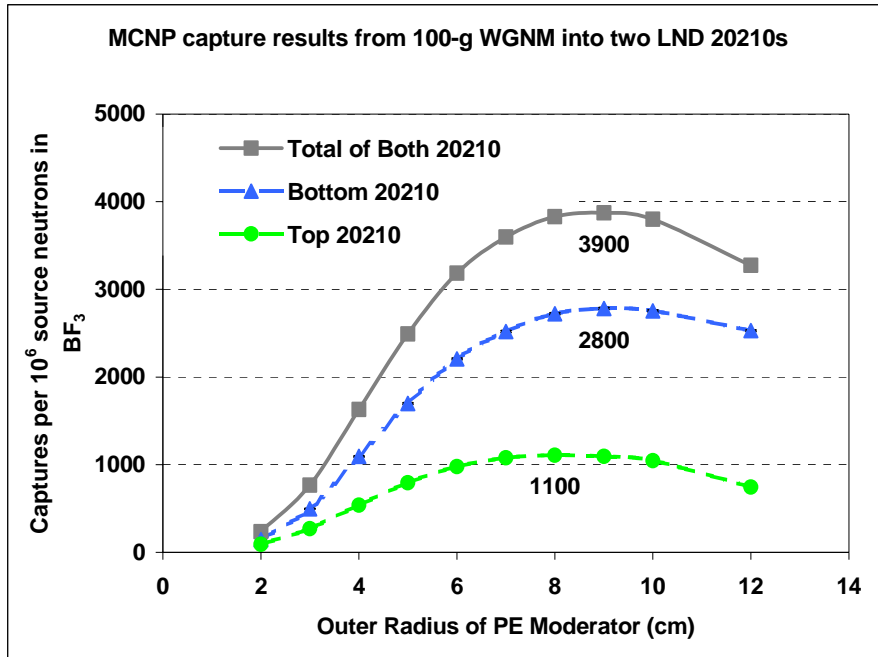


Fig 37. MCNP results for captures in LND 20210s located above and below a suitcase. The  $\text{BF}_3$ s were moderated by polyethylene and exposed inside a CTX 5500 to the suitcase containing a 100-g, 1-mm thick sheet of WGNM.

Figure 38 illustrates the significantly higher measured counts of the large active volume LND 20210 than the small active volume LND 201 to a given neutron source.

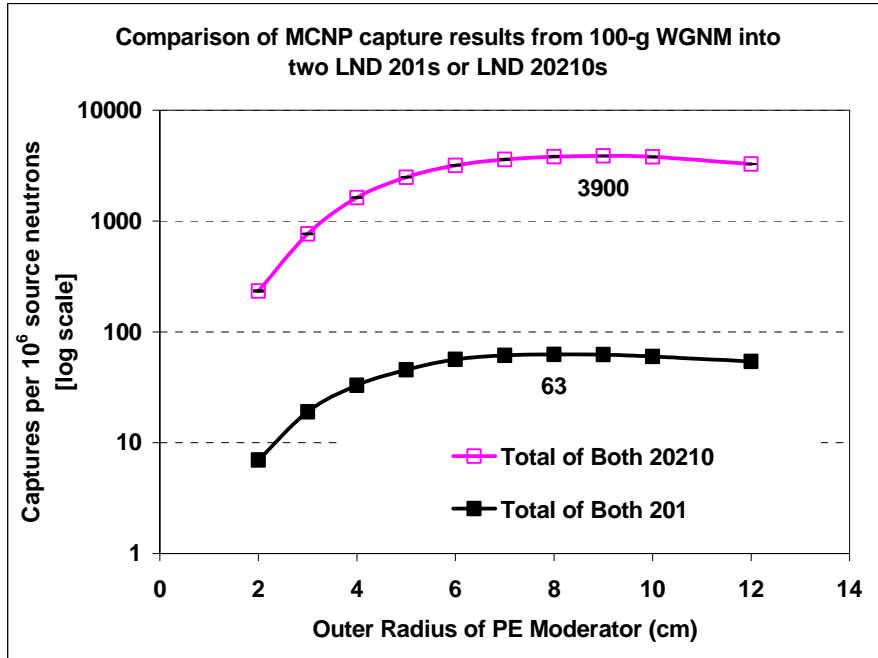


Fig 38. Comparison of MCNP results for captures in LND 201s versus LND 20210s. The  $\text{BF}_3$ s were moderated by polyethylene and exposed inside a CTX 5500 to the suitcase containing a 100-g, 1-mm thick sheet of WGNM.

Table 3 outlines the calculation of the expected counts in a 4-second interval in the BF<sub>3</sub>s. Laboratory measurements yielded a counts-per-second rate of background neutrons for each BF<sub>3</sub>. As expected, the LND 20210 has a higher background rate due to its larger active volume (111 cm<sup>3</sup> for the LND 20210 versus 6 cm<sup>3</sup> for the LND 201).

**Table 3. Calculation of Expected Background Counts for a BF<sub>3</sub> in a 4-Second Interval**

BF <sub>3</sub> Detector	Background Counts in 24-hr Interval per BF <sub>3</sub> [cts/sec]	Total Background Counts in 24-hr Interval (2 BF <sub>3</sub> ) [cts/sec]	Expected Background Counts (2 BF <sub>3</sub> ) In 4-Second Interval <sup>1</sup>
LND 201	0.03	0.06	0.2
LND 20210	0.26	0.52	2

<sup>1</sup> Based on CTX 5500 DS bag throughput of 384 bags hr<sup>-1</sup> over 4.4 m → results in bag velocity of 0.5 m s<sup>-1</sup> and suitcase residing in 2m section of SP Module for 4 seconds [www.invision-tech.com]

Table 4 outlines the calculation of the counts-to-background ratio for the small volume LND 201 BF<sub>3</sub>. The MCNP results from Figure 38 were multiplied by the specific yields for 100-g of WGNM from Table 1 to arrive at the counts per second of the BF<sub>3</sub>. The counts per second are multiplied by 4 seconds and compared to the expected background in that same 4-second interval from Table 3. The desired ratio of 10:1 was only achieved for a source of weapons-grade plutonium using the LND 201.

**Table 4. Calculations of Expected Counts to Background Ratio for the LND 201 BF<sub>3</sub>s**

LND 201	MCNP Measured Counts [cts/10 <sup>6</sup> n]	100-g Source n Based On Specific Yields [n/sec]	Expected Counts (2 BF <sub>3</sub> ) In 4-Second Interval	Expected Background Counts (2 BF <sub>3</sub> ) In 4-Second Interval	Counts To Background Ratio
Pu-239	63	3800	0.96	0.2	5 : 1
WGP		19400	4.9		20 : 1
U-235		0.1	2.5E-05		1E-04 : 1
WGU		3.1	7.8E-04		4E-04 : 1

Similarly, Table 5 outlines the calculation of the counts-to-background ratio for the large volume LND 20210 BF<sub>3</sub>. The desired ratio of 10:1 was achieved for a source of pure plutonium or of weapons-grade plutonium using the LND 20210.

**Table 5. Calculations of Expected Counts to Background Ratio for the LND 20210 BF<sub>3</sub>s**

LND 20210	MCNP Measured Counts [cts/10 <sup>6</sup> n]	100-g Source n Based On Specific Yields [n/sec]	Expected Counts (2 BF <sub>3</sub> ) In 4-Second Interval	Expected Background Counts (2 BF <sub>3</sub> ) In 4-Second Interval	Counts To Background Ratio
Pu-239	3900	3800	59	2	30 : 1
WGP		19400	303		150 : 1
U-235		0.1	1.6E-03		8E-04 : 1
WGU		3.1	4.8E-02		2E-04 : 1

## CONCLUSION

### Summary of Data

MCNP was used to model spherical  $\text{BF}_3$  detectors surrounded by spherical moderators. These calculations were used to obtain experience with the program using simple geometries and neutron sources. Results indicated that counting efficiency (i.e. captures in the  $\text{BF}_3$  gas) depended on the diameter of the spherical moderator and energy of the incident neutrons. In addition, these results showed that a shell of lead or carbon around the detector could extend the mean "lifetime" for a source neutron incident upon the moderator. For the spherical detectors, this increase in neutron "lifetime" resulted in increased measured counts in the  $\text{BF}_3$ .

Comparisons of MCNP-computations with laboratory measurements demonstrated that neutrons scattered from objects surrounding the detection system contribute significantly to the measured counts in the  $\text{BF}_3$  detector. In addition, these comparisons indicated that utilizing a sleeve of lead or of carbon might not provide an increase in measured counts in the  $\text{BF}_3$ . Since the measured results from cylindrical detectors contrasts the computations for spherical detectors, additional investigations are required before forming conclusions about the effectiveness of lead or carbon moderators.

Laboratory measurements showed that the count rates in the neutron detector from radiation background were extremely low. While these rates may be variable, analyses of background variations were not performed in this project. Background gamma radiation, while variable, occurred in channels that can be eliminated with a

discriminator that did not appreciably eliminate signals from neutron captures in the  $^{10}\text{B}$  gas of the  $\text{BF}_3$ .

Weapons-grade nuclear materials (WGNM) located in baggage would emit neutrons at rates well above background. Pu-239, weapons-grade plutonium (WGP), U-235, and weapons-grade uranium (WGU) are the most common WGNM for use in nuclear weapons. However, in the pure metal forms of Pu-239 and U-235, spontaneous fission occurs at rates so low that the emitted neutrons cannot easily be distinguished from background. Oxidation of the metals occurs readily and increases the yield of neutrons from  $(\alpha, n)$  reactions. However, in spite of this increase, the neutron yields from pure metals are so small that it would require very many large detectors to obtain measurable signals above background.

Normally, WGP or WGU are used in nuclear weapons rather than pure metals. Weapons-grade materials contain impurities (i.e. other isotopes) that have higher rates of spontaneous fission than pure Pu-239 or U-235. Using the large volume LND 20210  $\text{BF}_3$ , 100-g of Pu-239 was detected at 150 times the background rate and 100-g of WGP was detected at 30 times background. These results indicated that detection of WGP was five times more efficient than detection of Pu-239. Because of the low neutron emission rates, neither 100-g of U-235 or of WGU could be reliably be detected above background. Utilization of larger volume  $\text{BF}_3$  detectors and/or more detectors may enable detection above background.

## Considerations for Future Efforts

This project was intended to be the first step in determining the feasibility of reliably detecting small quantity weapons-grade nuclear materials. Future efforts should address the following considerations: selection and configuration of detectors; optimization of moderator material, size and configuration; increasing neutron yield; variability in neutron background; and selection of counting methods.

While proportional counters are favorable for thermal neutron detection, there are many manufacturers and sensitivities available beyond those used in this project. Consideration should be given to size and cost limitations in choosing a detector that maximizes measured neutron counts from a given source. Two detectors were placed above and below the WGNM but other configurations and more detectors may enhance the detection of smaller quantities. In conjunction with the detectors, consideration should be given to the material, size and configuration of the moderators. Large volumes of hydrogenated materials, such as the polyethylene modeled in this project, compete with the  $\text{BF}_3$  gas to capture thermal neutrons. Alternatives should be investigated, including the use of moderators with low thermal neutron capture cross-sections, such as carbon.

Neutron yields from WGNM increase as the fraction of Pu-239 or U-235 decrease, as they both have low spontaneous fission rates. Neutron yields may also be increased by actively causing fission to occur through the use of a pulsed neutron source. The source turns on to generate neutrons that then bombard the subject WGNM and induce fission. The source is then shut off in an interval to allow fission neutrons from the WGNM to be detected. While consideration of this active system is necessary, it

introduces significant radiation protection concerns and potentially costly shielding requirements.

Background neutron rates were measured as less than one count per second in the laboratory. Such low count rates, coupled with likely variation in the neutron background, prompt the need for further investigation into counting methods. Integrated counting, as used in this project, results in a count rate that may not account for the random time between background neutrons reaching the detector. Measuring one count per second, therefore, may just as likely be due to background neutrons as to source neutrons. Further consideration should be given to evaluating the time interval between counts measured in the detector. Neutrons produced from fissions in the source will have very short times between counts in the detector as compared to background neutrons.

Monte Carlo techniques, such as the Monte Carlo n-Particle (MCNP) code, are powerful tools that can be used to model scenarios that cannot feasibly be evaluated otherwise. The transport of a small quantity of weapons-grade nuclear material is one such scenario. The results of this project indicate that neutrons from a small quantity (100-g) of weapons-grade plutonium (WGP) may reliably be detected above expected background using larger volume  $\text{BF}_3$  detectors such as the LND 20210. Detection of 100-g of weapons-grade uranium (WGU), however, requires further investigation into detector size and configurations as discussed above.

## BIBLIOGRAPHY

**(Albright 1999)** Albright D, Barbour L, Gay C, Lowery T. Ending the production of fissile material for nuclear weapons: Background information and key questions. Table VI.4. Prepared by the Institute for Science and International Security, Washington, D.C. for the Fissile Material Information Workshop. Geneva, Switzerland; 25-26 January 1999. Available at: [http://www.isis-online.org/publications/fmct/primer/Section\\_VI.html](http://www.isis-online.org/publications/fmct/primer/Section_VI.html). Accessed 2 March 2002.

**(Allison 1996)** Allison GT, Cote OR, Falkenrath RA, Miller SE. Avoiding nuclear anarchy: Containing the threat of loose Russian nuclear weapons and fissile material. CSIA Studies in International Security; John F. Kennedy School of Government; Harvard University; 1996; Appendix B. Available at: [www.pbs.org/wgbh/pages/frontline/shows/nukes/readings/appendixb.html](http://www.pbs.org/wgbh/pages/frontline/shows/nukes/readings/appendixb.html). Accessed 3 March 2002.

**(Briesmeister 2000)** Briesmeister JF, ed. MCNP-A general Monte Carlo n-particle transport code. Version 4C. Los Alamos National Laboratory: LA-13709-M; March 2000.

**(Canberra 2002)** Canberra Industries. Neutron detection and counting. 2002. Available at: [http://www.canberra.com/literature/basic\\_principles/neutron.htm](http://www.canberra.com/literature/basic_principles/neutron.htm). Accessed 3 March 2002.

**(Cember 1996)** Cember H. Introduction to health physics. 3<sup>rd</sup> ed. New York: McGraw-Hill; 1996.

**(Chow 1993)** Chow BG, Solomon KA. Limiting the spread of weapon-usable fissile materials. RAND Distribution Services; RAND/DRR-377-USDP; 1993. Available at: [www.rand.org/publications/RB/RB7405/index.html](http://www.rand.org/publications/RB/RB7405/index.html). Accessed 4 March 2002.

**(DOE 1997)** U.S. Department of Energy. Final nonproliferation and arms control assessment of weapons-usable fissile material storage and excess plutonium disposition alternatives. January, 1997.

**(DOE 1998)** U.S. Department of Energy. Radiological safety training for uranium facilities. DOE-HDBK-1113-98; February 1998. Available at: <http://tis.eh.doe.gov/techstds/standard/hdbk1113/hdbk1113.pdf>. Accessed 4 March 2002.

**(DOE 2000)** U.S. Department of Energy. Guide of good practices for occupational radiological protection in uranium facilities. DOE-STD-1136-2000. Available at: <http://tis.eh.doe.gov/techstds/standard/std1136/std11362000.pdf>. Accessed 3 March 2002.

**(DOE 2001)** U.S. Department of Energy. Radiological safety training for plutonium facilities. DOE-HDBK-1145-2001; August 2001. Available at: <http://tis.eh.doe.gov/techstds/standard/hdbk1145/HDBK-1145-2001new.pdf>. Accessed 4 March 2002.

**(EPA 1990)** United States Environmental Protection Agency. Transuranium Elements: Volume 1, Elements of radiation protection. EPA 520/1-90-015. June 1990.

**(Harcourt 2002)** Harcourt, Inc. Academic Press Dictionary of Science and Technology. Available at: <http://www.harcourt.com/dictionary/def/6/9/0/7/6907200.html>. Accessed 18 April 2002.

**(IEER 1997)** Institute for Energy and Environmental Research. Physical, nuclear, and chemical properties of plutonium. February 1997. Available at: <http://www.ieer.org/fctsheets/ptu-props.html>. Accessed 3 March 2002.

**(IEER 2000)** Institute for Energy and Environmental Research. Physical, nuclear, and chemical properties of plutonium. August 2000. Available at: <http://www.ieer.org/fctsheets/uranium.html>. Accessed 3 March 2002.

**(InVision 2002)** InVision Technologies, 7151 Gateway Boulevard, Newark, CA 94560. Available at: <http://www.invision-tech.com/products/>. Accessed 4 March 2002.

**(Knoll 2000)** Knoll GF. Radiation detection and measurement. 3<sup>rd</sup> ed. New York: John Wiley & Sons, Inc.; 2000.

**(LND 2002)** LND, Inc., 3230 Lawson Blvd., Oceanside, NY 11572. February 2002. Available at: [www.lndinc.com](http://www.lndinc.com). Accessed 4 March 2002.

**(RSICC 2002)** Radiation Safety Information Computational Center, Oak Ridge National Laboratory, TN. SOURCES-4B, Code System for Calculating (alpha, n), Spontaneous Fission, and Delayed Neutron sources and Spectra. RSICC Code Package CCC-661 available for purchase at: <http://www-rsicc.ornl.gov/codes/ccc/ccc6/ccc-661.html>. Accessed 18 April 2002.

**(Shleien 1998)** Shleien B, Slaback LA, Birky BK, eds. Handbook of health physics and radiological health. 3<sup>rd</sup> ed. Baltimore, MD: Lippincott Williams & Wilkins; 1998.

**(Sublette 1997)** Sublette C. Nuclear weapons frequently asked questions. Section 6.0, The First Nuclear Weapons, 15 May 1997. The High Energy Weapons Archive. Available at: <http://www.fas.org/nuke/hew/Nwfaq/Nfaq8.html>. Accessed 3 March 2002.

**(Sublette 1999)** Sublette C. Nuclear weapons frequently asked questions. Section 8.0, Nuclear materials, 20 February 1999. The High Energy Weapons Archive. Available at: <http://www.fas.org/nuke/hew/Nwfaq/Nfaq6.html>. Accessed 3 March 2002.

**(Tsoulfanidis 1995)** Tsoulfanidis N. Measurement and detection of radiation. 2<sup>nd</sup> ed. Washington D.C.: Taylor & Francis; 1995: Chapter 14.

**(Turner 1995)** Turner JE. Atoms, radiation, and radiation protection. 2<sup>nd</sup> ed. New York: John Wiley & Sons, Inc.; 1995.